# Potato tuber *(Solanum tuberosum* L. cv Desiree) — characterization of starch interacting proteins and maltodextrin metabolism

Dissertation

zur Erlangung des akademischen Grades

"doctor rerum naturalium"

(Dr. rer. nat.)

in der Wissenschaftsdisziplin Biochemie

Junio Flores Castellanos

Ort und Tag der Disputation

Potsdam, 10.11.2023

eingereicht an der

Mathematisch-Naturwissenschaftlichen Fakultät

Institut für Biochemie und Biologie

der Universität Potsdam

Supervisor: Prof. Dr. habil. Joerg Fettke

Second Supervisor: Prof. Dr. Alisdair Fernie

Reviewers: Prof. Dr. Peter Geigenberger

Prof. Dr. Uwe Sonnewald

Published online on the
Publication Server of the University of Potsdam:
https://doi.org/10.25932/publishup-61505
https://nbn-resolving.org/urn:nbn:de:kobv:517-opus4-615055

# Declaration

I hereby declare that this thesis has been written on my own and without the use of sources and aids other than those indicated and cited within the text. This work has not been previously submitted to any examination authority in the same or a similar form.

Junio Flores Castellanos

Potsdam, 01.03.2023

# Abstract

Starch is a biopolymer for which, despite its simple composition, understanding the precise mechanism behind its formation and regulation has been challenging. Several approaches and bioanalytical tools can be used to expand the knowledge on the different parts involved in the starch metabolism. In this sense, a comprehensive analysis targeting two of the main groups of molecules involved in this process: proteins, as effectors/regulators of the starch metabolism, and maltodextrins as starch components and degradation products, was conducted in this research work using potato plants (*Solanum tuberosum* L. cv. Desiree) as model of study. On one side, proteins physically interacting to potato starch were isolated and analyzed through mass spectrometry and western blot for their identification. Alternatively, starch interacting proteins were explored in potato tubers from transgenic plants having antisense inhibition of starch-related enzymes and on tubers stored under variable environmental conditions. Most of the proteins recovered from the starch granules corresponded to previously described proteins having a specific role in the starch metabolic pathway. Another set of proteins could be grouped as protease inhibitors, which were found weakly interacting to starch. Variations in the protein profile obtained after electrophoresis separation became clear when tubers were stored under different temperatures, indicating a differential expression of proteins in response to changing environmental conditions.

On the other side, since maltodextrin metabolism is thought to be involved in both starch initiation and degradation, soluble maltooligosaccharide content in potato tubers was analyzed in this work under diverse experimental variables. For this, tuber disc samples from wild type and transgenic lines strongly repressing either the plastidial or cytosolic form of the α-glucan phosphorylase and phosphoglucomutase were incubated with glucose, glucose-6-phosphate, and glucose-1-phosphate solutions to evaluate the influence of such enzymes on the conversion of the carbon sources into soluble maltodextrins, in comparison to wild-type samples. Relative maltodextrin amounts analyzed through capillary electrophoresis equipped with laser-induced fluorescence (CE-LIF) revealed that tuber discs could immediately uptake glucose-1-phosphate and use it to produce maltooligosaccharides with a degree of polymerization of up to 30 (DP30), in contrast to transgenic tubers with strong repression of the plastidial glucan phosphorylase. The results obtained from the maltodextrin analysis support previous indications that a specific transporter for glucose-1-phosphate may exist in both the plant cells and the plastidial membranes, thereby allowing a glucose-6-

phosphate independent transport. Furthermore, it confirms that the plastidial glucan phosphorylase is responsible for producing longer maltooligosaccharides in the plastids by catalyzing a glucan polymerization reaction when glucose-1-phosphate is available. All these findings contribute to a better understanding of the role of the plastidial glucan phosphorylase as a key enzyme directly involved in the synthesis and degradation of glucans and their implication on starch metabolism.

# Zusammenfassung

Stärke ist ein Biopolymer, bei dem es trotz seiner einfachen Zusammensetzung schwierig ist, den genauen Mechanismus seiner Bildung und Regulierung zu verstehen. Verschiedene Ansätze und bioanalytische Instrumente können genutzt werden, um das Wissen über die verschiedenen am Stärkemetabolismus beteiligten Komponenten zu erweitern. In diesem Sinne wurde in dieser Forschungsarbeit eine umfassende Analyse durchgeführt, die auf zwei der wichtigsten Molekülgruppen abzielt, die an diesem Prozess beteiligt sind: Proteine als Effektoren/Regulatoren des Stärkestoffwechsels und Maltodextrine als Stärkebestandteile und Abbauprodukte, wobei Kartoffelpflanzen (*Solanum tuberosum* L. cv. Desiree) als Untersuchungsmodell dienten. Einerseits wurden Proteine, die physisch mit Kartoffelstärke interagieren, isoliert und mittels Massenspektrometrie und Western Blot analysiert, um sie zu identifizieren. Andererseits wurden die mit Stärke interagierenden Proteine in Kartoffelknollen von transgenen Pflanzen mit Antisense-Hemmung von stärkeverwandten Enzymen und in Knollen, die unter variablen Umweltbedingungen gelagert wurden, untersucht. Die meisten der aus den Stärkekörnchen gewonnenen Proteine entsprachen zuvor beschriebenen Proteinen, die eine spezifische Rolle im Stärkestoffwechselweg spielen. Eine andere Gruppe von Proteinen konnte als Proteaseinhibitoren gruppiert werden, die nur schwach mit der Stärke interagieren. Variationen im Proteinprofil nach der Elektrophorese-Trennung wurden deutlich, wenn die Knollen bei unterschiedlichen Temperaturen gelagert wurden, was auf eine unterschiedliche Expression von Proteinen als Reaktion auf wechselnde Umweltbedingungen hindeutet.

Da man davon ausgeht, dass der Maltodextrin-Stoffwechsel sowohl an der Entstehung als auch am Abbau von Stärke beteiligt ist, wurde in dieser Arbeit der Gehalt an löslichen Maltooligosacchariden in Kartoffelknollen unter verschiedenen experimentellen Variablen analysiert. Zu diesem Zweck wurden Knollenscheibenproben von Wildtypen und transgenen Linien, die entweder die plastidiale oder die cytosolische Form der α-Glucanphosphorylase und Phosphoglucomutase stark unterdrücken, mit Glucose-, Glucose-6-Phosphat- und Glucose-1-Phosphat-Lösungen inkubiert, um den Einfluss dieser Enzyme auf die Umwandlung der Kohlenstoffquellen in lösliche Maltodextrine im Vergleich zu Wildtyp-Proben zu bewerten. Relative Maltodextrinmengen, die durch Kapillarelektrophorese mit laserinduzierter Fluoreszenz (CE-LIF) analysiert wurden, zeigten, dass die Knollenscheiben Glukose-1-Phosphat sofort aufnehmen und zur Herstellung von Maltooligosacchariden mit

einem Polymerisationsgrad von bis zu 30 (DP30) verwenden konnten, im Gegensatz zu transgenen Knollen mit starker Unterdrückung der plastidialen Glukanphosphorylase. Die Ergebnisse der Maltodextrin-Analyse stützen frühere Hinweise darauf, dass ein spezifischer Transporter für Glucose-1-Phosphat sowohl in den Pflanzenzellen als auch in den plastidialen Membranen vorhanden sein könnte, was einen von Glucose-6-Phosphat unabhängigen Transport ermöglicht. Außerdem wird bestätigt, dass die plastidiale Glucanphosphorylase für die Herstellung längerer Maltooligosaccharide in den Plastiden verantwortlich ist, indem sie eine Glucanpolymerisationsreaktion katalysiert, wenn Glucose-1-Phosphat verfügbar ist. All diese Erkenntnisse tragen zu einem besseren Verständnis der Rolle der plastidialen Glucanphosphorylase als Schlüsselenzym bei, das direkt an der Synthese und dem Abbau von Glucanen und deren Auswirkungen auf den Stärkemetabolismus beteiligt ist.

# Publications

The results obtained during this research work were published in scientific journals:

- "The plastidial glucan phosphorylase affects the maltooligosaccharide metabolism in parenchyma cells of potato (Solanum tuberosum L.) tuber discs". (2022). **Castellanos, J. F**., & Fettke, J. Published in *Plant & cell physiology*, pcac174.

- "Gradual analytics of starch interacting proteins in developing potato (*Solanum tuberosum* L.) tubers further reveals that starch phosphorylation by glucan, water dikinase (GWD) and phosphoglucan, water dikinase (PWD) as well as the action of the plastidial glucan phosphorylase (PHO1) is essential during storage starch synthesis". **Flores-Castellanos J**., Khan, A., & Fettke, J. Under revision in *Plant Physiology and Biochemistry* since 20.02.2023.

In addition, contribution was done in the following publication:

- "Dpe2/phs1 revealed unique starch metabolism with three distinct phases characterized by different starch granule numbers per chloroplast, allowing insights into the control mechanism of granule number regulation by gene co-regulation and metabolic profiling". (2022). Li, X., Apriyanto, A., **Castellanos, J. F.,** Compart, J., Muntaha, S. N., & Fettke, J. Published in *Frontiers in plant science*, 13, 1039534.

# Acknowledgements

I want to express my gratitude to Prof. Dr. Fettke for giving me the opportunity to become part of the Biopolymer Analytics Group and each of the members that kindly supported me during my work. Special thanks to the Deutsche Akademischer Austauschdienst (DAAD) for funding me during the doctoral program and enabling me to achieve my goal.

I am infinitely grateful with my family for their unconditional support, especially my wife and kids for sharing every joy and challenge with me.

# List of figures

# List of tables

# Table of contents

# Abbreviations

| | |
|---|---|
| ADP | Adenosine diphosphate |
| AGPase | ADP-glucose pyrophosphorylase |
| APTS | 8-Aminopyrene-1,3,6-trisulfonic acid, trisodium salt |
| ATP | Adenosine triphosphate |
| BCA | Bicinchoninic acid |
| CE-LIF | Capillary electrophoresis with laser-induced fluorescence |
| DBE | Starch debranching enzymes |
| DP | Degree of polymerization |
| DPE1 | Disproportionating enzyme 1 |
| DTE | Dithioerythritol |
| EDTA | Ethylenediaminetetraacetic acid |
| ESV1 | Early starvation 1 |
| Fru | Fructose |
| Fru-6-P | Fructose-6-phosphate |
| GBSS | Granule bound starch synthase |
| Glc | Glucose |
| Glc-1-P | Glucose-1-phosphate |
| Glc-6-P | Glucose-6-phosphate |
| GPT | Glucose-6-phosphate/phosphate translocator |
| GWD | Glucan, water dikinase |
| HCCA | α-Cyano-4-hydroxycinnamic acid |
| HRP | Horseradish peroxidase |
| ISA1 | Isoamylase 1 |
| ISA2 | Isoamylase 2 |
| LDA | Limit dextrinase |
| LESV | Like-early starvation |
| LSF1 | Like sex four 1 |
| LSF2 | Like sex four 2 |

| | |
|---|---|
| m/z | Mass/charge ratio |
| MALDI-TOF | Matrix-assisted laser desorption/ionization-time of flight |
| MOS | Maltooligosaccharides |
| MS | Mass spectrometry |
| MS/MS | Tandem mass spectrometry |
| MW | Molecular weight |
| NAD | Nicotinamide adenine dinucleotide |
| NADP | Nicotinamide adenine dinucleotide phosphate |
| OD | Optical density |
| PAGE | Polyacrylamide gel electrophoresis |
| PGI | Phosphoglucoisomerase |
| PGM | Phosphoglucomutase |
| PHO | α-1,4 Glucan phosphorylase |
| PHO1 | Plastidial α-1,4 glucan phosphorylase |
| PHO2 | Cytosolic α-1,4 glucan phosphorylase |
| PTST1 | Protein targeting to starch 1 |
| PTST2 | Protein targeting to starch 2 |
| PWD | Phosphoglucan, water dikinase |
| SBE | Starch branching enzymes |
| SDS | Sodium dodecyl sulfate |
| SDS-PAGE | Sodium dodecyl sulfate- polyacrylamide gel electrophoresis |
| SEX4 | Starch excess 4 |
| SIP | Strong interacting proteins to starch |
| SSs | Starch synthases |
| Suc | Sucrose |
| Susy | Sucrose synthase |
| TFA | Trifluoracetic acid |
| UDP-glucose | Uridine diphosphate-glucose |
| v/v | Volume/volume |
| w/v | Weight/volume |

| | |
|---|---|
| WIP | Weak interacting proteins to starch |
| WT | Wild type |

# 1 Introduction

## 1.1 Starch

Starch is a carbohydrate polymer analogous to the animal glycogen, which is synthesized by plants and algae cells for energy storage and represents the main source of calories in the human diet (Tetlow et al., 2018). It is naturally produced as a highly ordered and dense packaging of glucans, leading to the formation of insoluble granules located in the chloroplast/amyloplast (Ball et al., 1996). The size, number, and morphology of these granules vary greatly depending on the species and even the organ analyzed (Tetlow et al., 2020). In grains and root tubers of staple foods such as wheat, potatoes, maize, rice, and cassava, starch is contained in large amounts.

Besides its importance as nutritional source, starch is widely used in industrial applications spanning engineering, food and beverages, textile, chemical, pharmaceuticals, and health, among others, due to its readiness to be modified into products having featured physicochemical characteristics (Adigwe et al., 2022).

### 1.1.1 Structure and composition

In plant cells, starch accumulates inside the stroma of the plastids as a complex granular structure made of two glucan polymers: amylose and amylopectin. Both polymers consist of α-1,4 linked glucose units, but opposite to amylose, which is basically a long linear glucose polymer, amylopectin contains a large number of relatively short glucan chains linked to each other through branches at α-1,6 positions (Tetlow et al., 2020) (Figure 1). Amylopectin, the major component, is responsible for the starch granule crystallinity achieved by its highly organized structure. This semi-crystalline property of the starch granules makes them insoluble in water (MacNeill et al., 2017). The linear α-glucan chains form clusters that extend from an amorphous lamella region, resulting in interacting longer chains that form double helices (Figure 1). Such organization can be mainly distinguished in two different arrangements or allomorphs denominated type A, B, as depicted in Figure 1 (Pérez et al., 2010; Apriyanto et al., 2022) and a C form containing a mixture of A and B allomorphs. In general, cereal endosperm starch exhibits the A-type allomorph, which is formed by shorter glucan chains that are packed in a uniform and dense way, and consequently, exclude more water (Figure 1) (Hizukuri et al., 1983; Imberty et al., 1988; McNeill et al., 2017). Plant leaves and tuber starches commonly exhibit the B-type form, which is composed of longer,

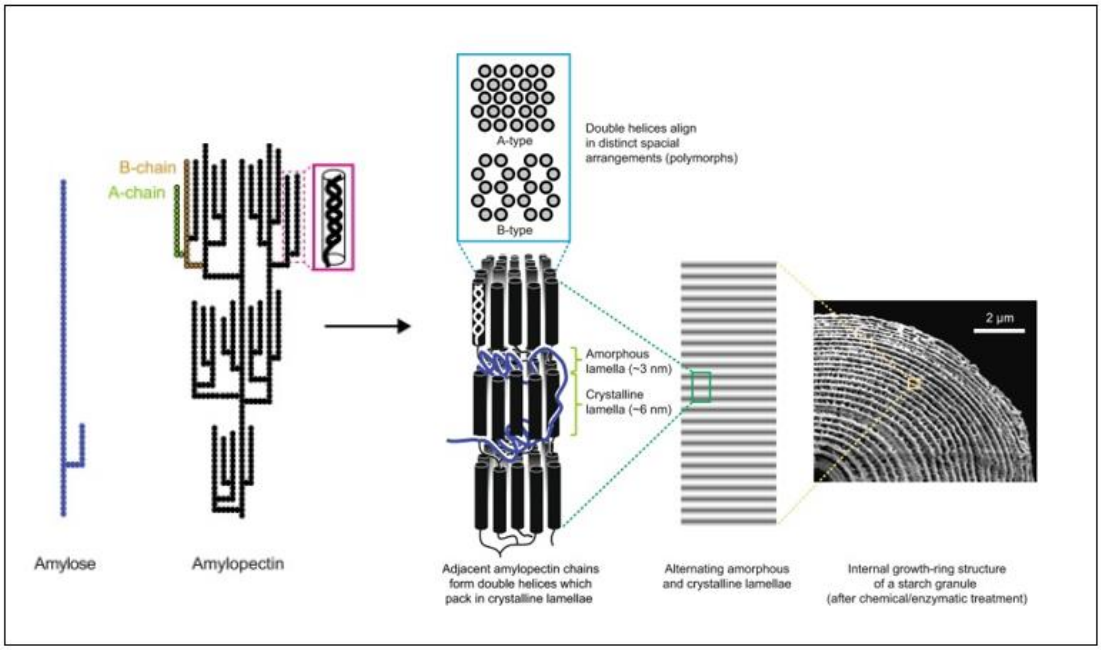


**Figure 1 Diagram model of the starch structure.** Representation of the amylose and amylopectin, and their arrangement in the conformation of the starch granule structure. Each circle within the amylose and amylopectin structures represents a glucose unit. Amylopectin is seen as a branched polymer leading to the formation of secondary structures in form of double helices. Each growth ring (right side of the arrow) has a thickness of ca. 200–400 nm and contains a semi-crystalline region and an amorphous region (Pfister et al., 2016). The semi-crystalline region consists of alternating crystalline lamellae (containing the linear glucan chains) and amorphous lamellae (containing most of the branch points) (Pfister et al., 2016). Based on the amylopectin adopted structure, the double helices cluster as densely packed A-type polymorph or less dense hexagonal B-type form. C-type polymorph is designated as a mixture of A and B. Adapted from Pfister et al. (2016). Copyright American Society of Plant Biologists.

more dispersed α-glucan chains that form a hexagonal-shape frame, allowing for more water incorporation (Figure 1) (Imberty et al., 1988; Tetlow et al., 2020). The C- type organization is designated to the starch granules that can be found in cassava (*Manihot esculenta* L.), banana (*Musa sp*.) fruits, and legume species (Bogracheva et al., 1998; Buléon et al., 1998; Zhang et al., 2012).

Starch granules contain in addition non-carbohydrate material such as proteins (0.1- 0.7% by weight, mostly in the form of enzymes involved in starch metabolism), lipids, phosphate (linked covalently to the glucans), and trace quantities of minerals (Pérez et al., 2010).

### 1.1.2 Transitory and storage starch

Depending on the time cycle regarding the starch synthesis and degradation, as well as its biological function, starch can be classified as transitory and storage starch. In photosynthetic tissues like plant leaves, starch is synthesized in the chloroplasts of mesophyll cells during the day and remobilized at night to provide carbon and energy for maintenance and growth (Stitt et al., 2012). These short-term reserves, known as transitory starch, are formed directly from intermediates of the Calvin-Benson cycle in presence of light and is degraded during the night to provide substrates for respiration in the leaf and for the synthesis of sucrose (Suc) that can be exported to growing sink organs. On the other side, storage starch is synthesized from the imported Suc in specialized amyloplasts of non-photosynthetic tissues like tubers, roots and seeds and is stored over a long period of time. Remobilization of this storage starch takes place during seed germination, tuber sprouting, or regrowth, when photosynthesis has either not yet resumed or is insufficient to meet the demand of energy and carbon skeletons (Lloyd et al., 2015; Santelia et al., 2017).

### 1.1.3 Starch biosynthesis

Starch biosynthesis is a complex mechanism that involves the coordinated activity of several groups of enzymes. From a general perspective, the major groups of enzymes involved in starch synthesis, each with various specific isoforms, can be classified in starch synthases (SSs, EC 2.4.1.21), starch branching enzymes (SBEs, EC 2.4.1.18) and starch debranching enzymes (DBEs, 3.2.1.41) (Tetlow et al., 2020; Merida et al., 2021; Shoaib et al., 2021).

Besides the afore mentioned core groups of proteins, other enzymes with essential activities in the starch biosynthesis take part. ADP-glucose pyrophosphorylase (AGPase, EC 2.7.7.27) is, for instance, the key enzyme on the first steps of starch synthesis which produces ADP-

glucose (ADP-Glc) from glucose-1-phosphate (Glc-1-P) and adenosine triphosphate (ATP). ADP-Glc is the substrate used by the SSs to extend the α-1,4 linked glucans. Five main isoforms of SSs are essentially found in all crops, namely SS1, SS2, SS3, SS4, and granule bound starch synthase (GBSS or WAXY). The latest is the most prominent in the starch granule comprising up to 95 % of the starch bound proteins (Helle et al., 2018). Among these, SS1, SS2, and SS3 are involved in the synthesis of amylopectin (Delvallé et al., 2005; Zhang et al., 2008) whereas GBSS is involved in amylose synthesis, as it has been demonstrated that GBSS knockout mutants produce amylose-free starch (Nakamura et al., 1995; Toinga-Villafuerte et al., 2022). Recently, a protein named protein targeting to starch 1 (PTST1) was discovered to target GBSS to the starch granules (Seung et al., 2017).

SBE are responsible for the trimming of α-1,4 glucan chains transferring segments to an acceptor chain to introduce branching points through α-1,6 linkages. The neighboring glucan chains originated from the branching points form double helix structures packed into stable semi-crystalline lamellae form (Streb et al., 2014). Considering this, investigations on the different SBE isozymes indicate that each of them have a particular role in the formation of the fine amylopectin structure (Sawada et al., 2018). DBEs, in counterpart to SBE, hydrolyze the α-1,6 glycosidic bonds releasing glucan chains. In this way, DBE also contribute to the proper amylopectin structure arrangement promoting its crystallization. DBE can be classified in two classes: isoamylase (ISA) and limit-dextrinase (LDA) (Streb et al., 2014). ISA1 and ISA2 take part in the amylopectin biosynthesis, whereas ISA3 and LDA participate in the starch degradation (Delatte et al., 2006; Lin et al., 2013; Streb et al., 2014).

A set of enzymes (i.e., GWD, PWD, LSF1, LSF2 and SEX4) are involved in the starch degradation by regulating and promoting the phosphorylation/dephosphorylation of glucans (Helle et al., 2018). Early starvation protein 1 (ESV1) and its homologue like-early starvation protein (LESV), both proteins found associated to the Arabidopsis starch granules, are also related to the starch degradation by modulating the organization of starch and consequently, affecting the glucan accessibility to catabolic enzymes (Singh et al., 2022).

Other proteins, presumably lacking catalytic activity, are crucial in the different phases of the starch formation and degradation process. *A. thaliana* starch synthase 5 (SS5), for instance, participates in the regulation of the morphology and starch granule number in the chloroplasts, although lacking the glycosyltransferase activity associated with the SSs (Abt et al., 2020). Similarly, Seung et al. (2017) showed that the protein targeting to starch 2 (PTST2) interacts with SS4 in Arabidopsis plants, and its suppression causes a phenotype

similar to SS4 mutants, where a reduced number of starch granules is observed in comparison to wild type plants.

As described above, the number of enzymes involved in the starch biosynthesis and degradation is extensive. To date, data of the complete set of proteins with the exact implication on starch metabolism is far from being totally described. However, in the last years, significant progress has been achieved through genome sequencing of many plant species and comparing the data with formerly well characterized organisms, seeking for homologous transcripts of starch-related genes. Along transcripts comparison, proteomic approaches have strongly supported the identification of several starch-associated enzymes as well as many putative novel isoforms. Various investigations focused on the analysis of proteins that remain in association with the starch granules have been conducted mainly in storage starch of crop species including maize, wheat kernels, rice endosperm, and potato tubers, among others (Grimaud et al., 2008; Bancel et al., 2009; Xing et al., 2016; Helle et al., 2018, 2019). However, little attention has been given to the analysis of the whole starch proteome under different physiological scenarios, what could eventually allow the disclosure of additional enzymes implicated in the starch metabolism and their role under specific conditions.

### 1.2 Synthesis of starch in potato tuber (*Solanum tuberosum* L.)

Starch is the major component of potato tubers, which makes the *S. tuberosum* L. specie an ideal plant model to investigate the multiple open questions regarding the starch metabolism. In 2014, a web resource named Spud DB Potato Genomic Resource (plantbiology.solanaceae.msu.edu) was created by the Potato Genome Sequencing Consortium with the aim to provide a centralized access to the potato genome sequences and associated annotation datasets (Hirsch et al., 2014). This database enables the consulting of transcripts and predicted protein sequences, among other resources. In this context, conducting a genome-wide analysis seeking for genes associated to the starch metabolism in potato, Van Harsselaar et al. (2017) identified 77 loci encoding enzymes associated to this process with numerous novel putative isoforms. Transcriptome analysis enabled them to differentiate between leaf and tuber specific isoforms of starch genes, finding for instance, a high expression of Susy4 and SS5 in tuber, whereas BAM3.1 (a β-amylase) and AMY1.1 an (α-amylase), were found highly expressed in leaves.

In tubers, starch is synthesized in the amyloplasts, and it relies on the translocation of metabolites from the cytosol through the amyloplast envelope (Hofius et al., 2007). This process initiates with the import of sucrose (Suc) through the phloem into the sink organ and cells, thus into parenchyma cells (Figure 1.1) (Turgeon et al., 2005; MacNeill et al., 2017). However, evidence suggests that a direct transport of Glc-1-P from the potato tuber apoplast to the amyloplast for the synthesis of starch is also possible (Fettke et al., 2010) (Figure 1.1). Later, in the cytosol, Suc is cleaved by sucrose synthase (Susy; EC 2.4.1.13) to produce UDP-glucose and Fructose (Fru). The end products of Suc degradation will enter the hexose phosphate pool, which consists of a mixture of Fru-6-P, Glc-6-P and Glc-1-P. In the current storage starch biosynthesis model, outlined in Figure 1.1, Glc-6-P is imported into the amyloplast by glucose-6-phosphate/phosphate translocator (GPT) (Kammerer et al., 1998). Once inside the amyloplast, Glc-6-P is reconverted into Glc-1-P by the plastidial PGM to serve as substrate for starch synthesis. The destination that Glc-1-P follows in the potato amyloplast can be diverse. It can be converted to ADP-glucose by AGPase to serve as substrate for starch synthases (SSs; EC 2.4.1.21), which transfer glucosyl residues to α-glucan chains. In an alternate biosynthetic route model, the plastidial α-1,4 glucan phosphorylase (PHO1) mediates the transfer of glucose units to native starch granules using the Glc-1-P as substrate (Fettke et al., 2010). Other models consider that Glc-1-P might be used by PHO1 to add glucosyl units to the non-reducing end of α-glucan chains, creating longer linear maltodextrins which can in turn be used for starch synthesis through the synchronized action of SSs and SBEs (Shoaib et al., 2021). However, under normal physiological conditions, the ADP-glucose dependent pathway for starch biosynthesis is clearly dominant considering that *S. tuberosum* L. transgenics plants having antisense repression of PHO1 showed no significant influence on starch accumulation, neither in leaves nor tubers (Sonnewald et al., 1995). The Glc-1-P dependent pathway mediated through PHO1, in counterpart, is more effective in potato tubers at 20 °C or lower temperature (Fettke et al., 2012; Orawetz et al., 2016).

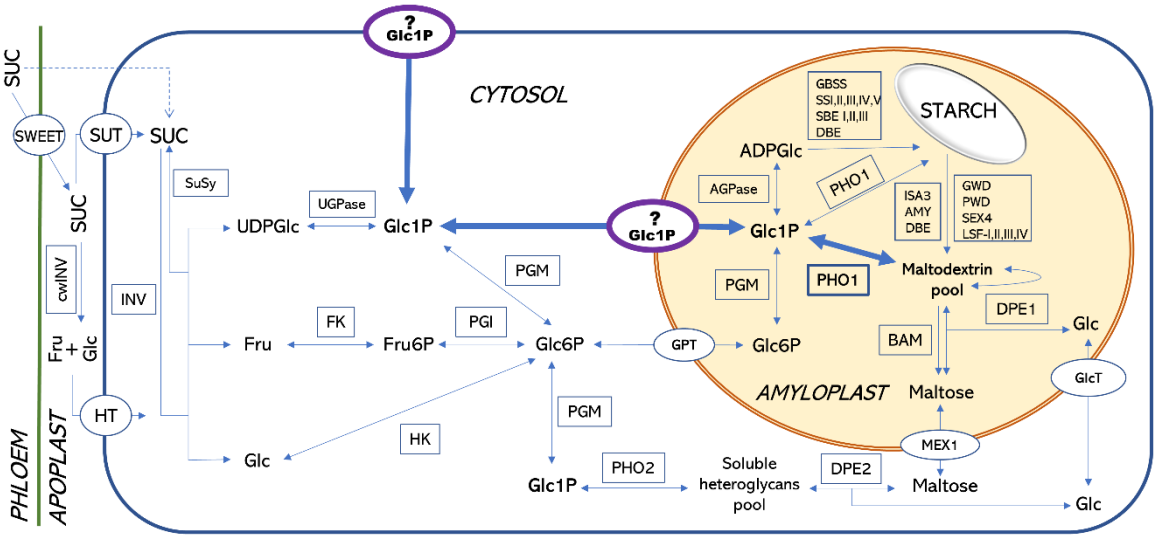


**Figure 1.1 Starch metabolic pathway in potato tuber (Flores-Castellanos et al., 2022).** For reserve starch accumulation in sink organs, photosynthesis derived Suc is apoplastic loaded into the phloem for tuber translocation (Braun et al., 2014). Suc can be unloaded in the apoplastic space facilitated by sugar transporters like SWEET, and then loaded into the parenchyma cells by SUT or via hexose transport proteins (HT) after being hydrolyzated by *cw*INV (Koch, 1996; Proels et al., 2014; Fernie et al., 2020). Alternatively, Suc enters symplastically the tuber parenchyma cells via plasmodesmata (dashed arrow) (Chen, 2014; Julius et al., 2017; Fernie et al., 2020). Once Suc has reached the sink cell, it is hydrolyzed by INV into Glc and Fru, or degraded by SuSy into UDP-glucose and Fru. Glc-1-P is then produced either from UDP-glucose by AGPase, or from Glc-6-P interconversion mediated by the cytosolic PGM. When Glc-1-P is externally supplied, it can be taken up by tuber cells and enter two paths: a) it is metabolized in the cytosol via PHO2 by transferring the glucosyl residue to soluble heteroglycans (Fettke et al., 2008); b) it is directly transported into the amyloplasts and, through a PHO1 dependent action, is destined to the starch (Fettke et al., 2010, 2012). The different routes that Glc-1-P might follow inside the amyloplast before being incorporated into the potato tuber starch are depicted.

SUC, sucrose; SUT, sucrose transporter; cwINV, cell-wall invertase; HT, hexose transporter; INV, invertase (cytosolic); SuSy, sucrose synthase; UGPase, UDP-glucose pyrophosphorylase; AGPase, ADP-glucose pyrophosphorylase; BT1, adenine nucleotide transporter BT1 (Kirchberger et. al, 2007); PGM, phosphoglucomutase; GBSS, granule-bound starch synthase; SSI-V, starch synthases; SBEI-III, starch branching enzymes; DBE, debranching enzyme; PHO1; plastidial glucan phosphorylase; PHO2, cytosolic glucan phosphorylase; GWD, α-glucan, water dikinase; PWD, phosphoglucan, water dikinase; SEX4, starch excess 4; ISA1-3, isoamylase 1, 2 and 3; AMY, α-amylase; DPE1 and DPE2, disproportionating enzyme 1 and 2; BAM, β- amylase; GlcT, glucose transporter (Cho et al., 2011); MEX1, maltose exporter; GPT, glucose-6-phosphate/phosphate translocator (Kammerer et al.,1998); HK, hexokinase; FK, fructokinase; PGI, phosphoglucoisomerase.

### 1.3 α-1,4 Glucan phosphorylase

α-1,4 glucan phosphorylase (PHO; EC 2.4.1.1) is an enzyme possessing both glucan-synthesizing and glucan-degrading activity and therefore, closely connected to the starch metabolic pathway (Albrecht et al., 2001). In the phosphorolytic reaction, PHO produces Glc-1-P from an α-1,4 linked glucan chain in presence of inorganic phosphate, as it is depicted in Figure 1.2. In the reverse reaction (synthesis) PHO catalyzes the addition of glucosyl units from Glc-1-P to the non-reducing end of an α-1,4 linked glucan chain, releasing inorganic phosphate (Figure 1.2). Even though a first report indicating the relation of PHO with the metabolism of starch exists since 1940 (Hanes, 1940), the exact role that this enzyme and its different isoforms might perform in the plants *in vivo* in relation to the starch and carbohydrate metabolism is still a matter of investigation.

In plants, there are two compartment-specific forms of glucan phosphorylases. One isoform, designated as PHO1, PHS1 or PhoL, is expressed in the chloroplast/amyloplast. This isoform is characterized for having low affinity towards branched glucans like glycogen (therefore named PhoL), acting preferentially on linear low-molecular-weight glucans (Steup, 1988; Fettke et al., 2004). On the other side, the cytosolic form of the glucan phosphorylase is called PHO2, PHS2 or PhoH and is characterized for possessing high affinity towards glycogen and acting on cytosolic heteroglycans (Steup, 1990; Fettke et al., 2005; Lin et al., 2017). Despite a difference in the molecular size, both isoforms present highly conserved regions. PHO1 contains an extra peptide of up to 82 amino acid residues (known as L80 domain) in the middle of its sequence that is missing in the cytosolic forms of higher plant phosphorylases (PHO2) (Tickle et al., 2009; Hwang et al., 2020; Shoaib et al., 2021). This prominent peptide can be distinguished in yellow-red color in Figure 1.2 (B), where the tertiary structure of PHO1 and PHO2 is represented. Different attributions have been proposed to this domain. It is believed, for instance, that it might sterically hinder the binding of PHO1 to large polysaccharides and it could be related to the various biochemical functions of PHO1 in potato plants (Cuesta-Seijo et al., 2016; Shoaib et al., 2021). Other authors remark that the L80 domain contains a set of negatively charged amino acids and potential phosphorylation sites, which are indications of a putative regulatory role within the enzyme (Hwang et al., 2020). In addition, a PEST motif (rich in proline, glutamic acid, serine, and threonine), which is a potential substrate for proteasome-mediated degradation, has been observed in the L80 domain of different plant species. (Hwang et al., 2020; Shoaib et al., 2021).

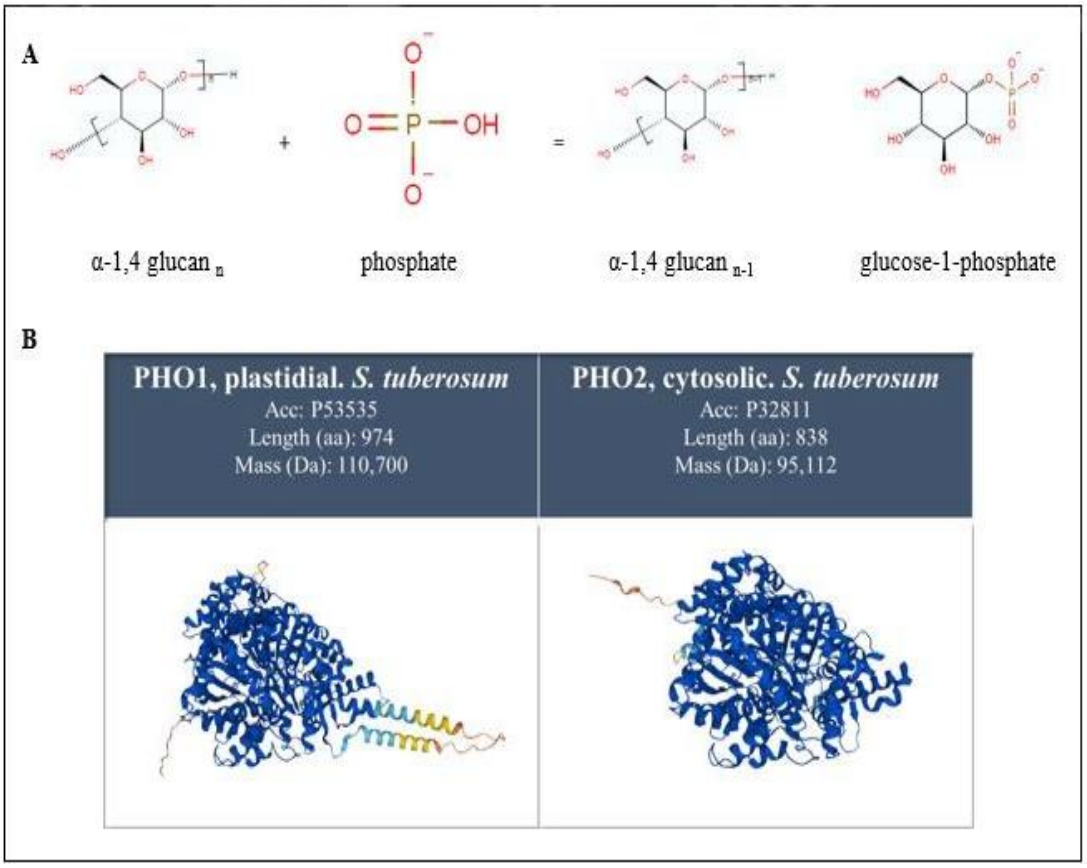


**Figure 1.2 Scheme of the reaction catalyzed by α-1,4 glucan phosphorylase (PHO)**. **A**. In presence of inorganic phosphate, PHO catalyzes the phosphorolytic cleavage of a glucose unit from an α-1,4 linked glucan, producing a molecule of Glc-1-P. It also acts in a reverse reaction (synthesis) adding glucosyl units to an α-1,4 linked glucan using Glc-1-P as substrate, releasing inorganic phosphate. Adapted from Uniprot (https://uniprot.org). **B**. Tertiary structure of the plastidial PHO1 and cytosolic PHO2 from potato (*S. tuberosum* L.). A prominent peptide (yellow-red color) known as L80 peptide can be distinguished in the chloroplastic isoform PHO1, which is absent in the cytosolic isozyme.
Prediction of the three-dimensional protein structures were obtained from AlphaFold (https://alphafold.ebi.ac.uk/).

## 1.4 Phosphoglucomutase

Phosphoglucomutase (PGM; EC 5.4.2.2) is an essential enzyme in the metabolism of carbohydrates that similarly to PHO, exists in plants as plastidial and cytosolic forms. PGM catalyzes the interconversion of Glc-6-P and Glc-1-P (Figure 1.3), which represents a central metabolic step with respect to the further carbon destination (Egli et al., 2010). Glc-6-P is used in the glycolysis pathway, whereas Glc-1-P is utilized in the synthesis of glucan polymers such as starch or cell wall structures (Guedon et al., 2000; Fernie et al., 2002). PGM, together with PGI (phosphoglucoisomerase), the enzyme responsible for Glc-6-P and Fru-6-P (Fructose-6-Phosphate) interconversion, are thought to keep the hexose phosphate pool in equilibrium when the carbon demands through the principal metabolic pathways change (Egli et al., 2010; Fernie et al., 2001; Hofius et al., 2007). In developing potato tubers, such equilibrium is maintained with Glc-6-P being the most abundant form of the hexose phosphates, which is found in a proportion of six to ten mol of Glc-6-P per mol of Glc-1-P, and the equivalent of three to four mol per mol of Fru-6-P (Tauberger et al., 2000; Fernie et al., 2002). It has been demonstrated that potato plants lacking either the plastidial or cytosolic isoform of PGM have a considerable reduction in starch formation in leaves and storage organs (Tauberger et al., 2000). Similarly, lack of the entire PGM activity in transgenic Arabidopsis plants caused low accumulation of starch and were distinguished by a dwarf phenotype and for being impeded to develop functional flowers and seeds (Malinova et al., 2014).

Additional evidence contributing to the relevance of PGM in the starch metabolic pathway was demonstrated by Wang et al. (2022) who overexpressed the plastidial isoform of the sweet potato (*Ipomoea batata)* PGM in a sweet potato cultivar characterized for its low starch content, observing a significant increase of the starch content in the transgenic sweet potatoes compared with wild type.

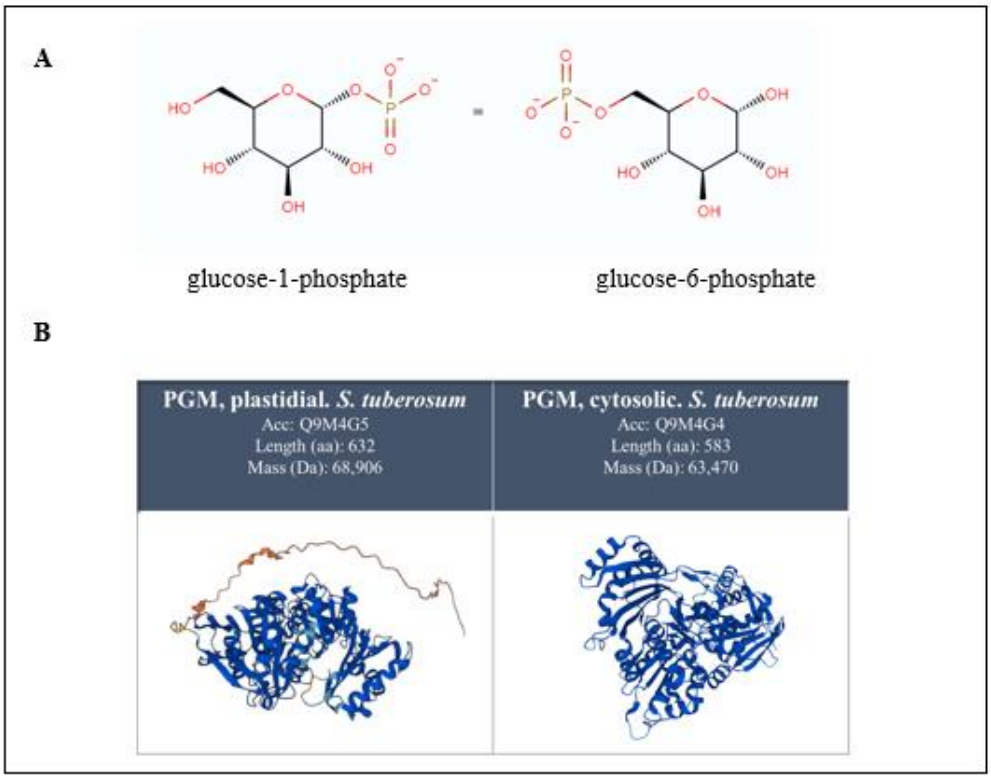


**Figure 1.3 Scheme of the reaction catalyzed by phosphoglucomutase (PGM). A.** PGM catalyzes the interconversion of Glc-1-P and Glc-6-P using $Mg^{+2}$ ion as cofactor. It is believed that PGM operates near to the equilibrium, maintaining a ratio of circa 10 mol of Glc-6-P per mol of Glc-1-P in potato tuber (Tauberger et al., 2000). **B.** Tertiary structure of *S. tuberosum* L. plastidial PGM and cytosolic PGM. Predicted 3D structures were obtained from AlphaFold web resource.

## 1.5 Glucose-1-phosphate as key substrate in starch and maltooligosaccharide metabolism

Glc-1-P is a central metabolite in the carbohydrate and starch metabolic pathway. Its synthesis is mostly regulated by PGM, the enzyme responsible for keeping the hexose phosphate pool in equilibrium. In potato tuber cells, Glc-1-P is found in considerably lower amount than Glc-6-P, which is considered the main precursor that is transported into the amyloplast for the synthesis of starch (Tauberger et al., 2000). In potato tubers, conversion of Glc-6-P into Glc-1-P is a crucial step in the starch biosynthesis. As proof, transgenic potato plants repressing the plastidial PGM resulted with a strong reduction of starch in the tubers (Tauberger et al., 2000; Fernie et al., 2002). The same effect was observed in transgenic lines repressing the cytosolic PGM. Moreover, inhibition of the plastidial PGM activity caused increased amounts of Suc and hexose phosphates (Tauberger et al., 2000). Nevertheless, when transgenic potato plants were generated having a simultaneous repression of both the plastidial and cytosolic PGM, unexpectedly the starch levels were recovered approaching to the wild type plants (Fernie et al., 2002). This result clearly indicated that additional carbon fluxes toward starch occur. In this regard, the direct transport of Glc-1-P into the plastids was proposed as the probable mechanism to overcome the inhibition of starch synthesis forced by the simultaneous repression of the two PGM isoforms (Fernie et al., 2002; Fettke et al., 2008). Evidence supporting this assumption was demonstrated by Fettke et al. (2010) who showed that potato tuber discs incubated with $^{14}C$ labelled Glc-1-P were able to incorporate this hexose phosphate into the starch at higher rate than Glc-6-P, Glc, or Suc. Nevertheless, when using transgenic potato lines with a reduced activity of the plastidial phosphorylase isozyme, starch labelling was significantly diminished. Further, a reduction of the PGM activity revealed no effect on the starch labelling (Fettke et al., 2010). These findings strongly supported the hypothesis that a putative Glc-1-P transporter exists within the cell and amyloplast membrane of the parenchyma cell of potato tubers for the direct transport of this metabolite and further utilization during the synthesis of starch. Also, it can be assumed that PHO1 plays a significant role in the starch biosynthesis by using the available Glc-1-P to elongate glucan chains which could then be used in the starch formation. Other possible explanation is that glucosyl units were directly incorporated into the starch surface by the action of PHO1. Besides the indications of a direct transport of Glc-1-P towards the amyloplasts, there is an evident gap whether Glc1-P also affects the cellular MOS metabolism. It is believed that

PHO1, in coordination with the disproportionating enzyme 1 (DPE1; EC:2.4.1.25), which is a plastidial α 1,4 glucanotransferase, use Glc-1-P for the synthesis of maltooligosaccharide (MOS) primers, thus contributing to the very early stage of the starch granule formation (Lin et al., 2017).

# 2 Aim of the project

The characterization of the starch proteome is fundamental in revealing part of the set of enzymes that participate in the metabolism of starch. It could provide hints on the determination of the activities carried out by the enzymes which are found physically interacting with the starch granules in the formation, regulation, and degradation of this essential polymer. In the last years, increasing number of plastidial proteins conserved among plant species and with so far unspecified function have been predicted through bioinformatic analysis as putative starch-related proteins. A possible identification, analysis, and exact location of these new and previously identified proteins within the starch granule will contribute on elucidating their function and possible synergy with other starch-related enzymes.

On the other side, although it has been demonstrated that the plastidial glucan phosphorylase enzyme has a strong implication on the carbohydrate and starch metabolism, its role on the metabolism of glucans has not been profoundly investigated. For the formation of storage starch, it is traditionally considered that Glc-6-P is the form of carbon source that enters the amyloplasts to be later converted to Glc-1-P by the plastidial phosphoglucomutase, serving Glc-1-P as precursor for the formation of starch. However, using Glc-1-P labelled with radioisotope carbon 14, Fettke et al. (2010) demonstrated the capability of potato tuber discs to directly incorporate Glc-1-P into starch when tuber discs samples were incubated with this substrate. Thus, a viable alternate route for starch biosynthesis was revealed.

With these precedents and making use of bioanalytical methods, this project aims the extraction, characterization and profiling of proteins that are found interacting with the potato tuber starch. Also, the strength of the interaction is evaluated based on the way the different proteins can be isolated from starch.

In addition, this work purposes a comprehensive analysis of the maltooligosaccharide metabolism in potato tubers to get insights on how these metabolites are regulated and to which extent can be altered when tuber samples are incubated on different experimental solutions containing glucose or glucose-phosphates. By this mean, putative cell transporters besides the already described for Glc-6-P is investigated. At the same time, the precise implication of the glucan phosphorylase isozymes and phosphoglucomutase on the maltodextrin regulation is assessed by the incubation of parenchyma tuber tissue of transgenic plants repressing the activity of these enzymes with the experimental solutions.

# 3 Materials and methods

## 3.1 Biological material

### 3.1.1 Potato plants

Potato wild type plants (*S. tuberosum* L. cv. Desiree), transgenic lines expressing an antisense construct against both plastidial phosphorylase isozymes (PHO1a + b, for details see Fettke et al., 2005) or possessing a reduced expression of the cytosolic phosphorylase isozyme (PHO2; Fettke et al., 2005) and transgenic lines with a lowered expression of both cytosolic and plastidial phosphoglucomutase (PGM) (Lytovchenko et al., 2002; Fettke et al., 2008), were grown under controlled conditions (12 h light period at 300 µE $m^{-2}$ $s^{-1}$, 22°C) in a grow chamber. Potato tubers were harvested after 3 months and stored in the dark at room temperature, except where otherwise stated.

## 3.2 Chemicals and enzymes

All enzymes and chemicals were purchased from Sigma-Aldrich (Steinheim, Germany), Merckmillipore (Tullagreen, Ireland), Roche (Mannheim, Germany), Biorad Laboratories (München, Germany), Duchefa Biochemie (Haarlem, Netherlands) and Carl Roth GmbH + Co. KG (Karlsruhe, Germany).

## 3.3 Methods

### 3.3.1 Starch isolation from potato tuber

Potato tubers were peeled and homogenized in 100 mL of cold distilled water per 10- 15 g of tuber material using a blender. The mixture was filtered through a 100 µm net sieve and passed into 50 mL Falcon tubes. Sample tubes were kept on ice for 1 h to allow the starch to settle down. Supernatant was discarded and the starch pellet was resuspended with 40 mL cold distilled water, vortexed and centrifuged at 1500 g for 3 min. Supernatant was discarded and this washing procedure was repeated three times. Finally, starch samples were freeze dried.

### 3.3.2 Screening of transgenic potato plants

#### 3.3.2.1 Extraction of buffer-soluble proteins

250 mg tuber material without periderm was homogenized in 0.3 mL precooled grinding buffer (100 mM HEPES-NaOH, pH 7.5, 1 mM EDTA, 2 mM DTE, 10% (w⁄v) glycerol) using an Ultra-Turrax. After centrifugation (20, 000 g, 10 min, 4°C), 120 µL supernatant containing the soluble proteins were recovered and used for protein quantification and native PAGE separation.

#### 3.3.2.2 Quantification of buffer-soluble proteins

Buffer-soluble proteins were quantified using the Bradford (1976) microassay with known concentrations of bovine serum albumin as standard.

#### 3.3.2.3 Detection of phosphorylase activity by native PAGE

20 µg buffer-soluble proteins were separated under no-denaturing conditions through a native PAGE discontinuous gel using a 7.5% (w/v) total monomer concentration and 0.2 % (w/v) glycogen from oyster in the separation gel (Sigma-Aldrich® Product No. G8751) (Steup, 1990). The stacking gel was prepared mixing 1 mL of 0.5 M Tris- phosphate buffer (pH 7.3), 2 mL of acrylamide/bisacrylamide 37, 5:1.2 solution, 2 mL of 0.2 mM riboflavin and 3 mL distilled water. The stacking gel solution was used to overlay the separation gel and photopolymerized with UV light. A pre-cooled 38 mM glycine-Tris (pH 8.5) solution was used as running buffer. Electrophoresis was performed at 4 °C under constant voltage (250 V) and current (40 mA). Following electrophoresis, the separation gel was incubated in 50 mL 100 mM citrate-NaOH (pH 6.5) solution during 10 min. Later, the solution was discarded and replaced with a 100 mM citrate-NaOH/ 20 mM Glc-1-P (pH 6.5) solution during 30- 60 min and then stained with an iodine solution made of 0.23% (w/v) KI and 0.13% (w/v) $I_2$ (Malinova et al., 2014).

#### 3.3.2.4 Detection of phosphoglucomutase activity by native PAGE

A native PAGE was performed following the procedure described by Egli et al. (2010). The separation gel contained 6% (w/v) acrylamide (30:0.8 acrylamide: bis-acrylamide) and 375 mM Tris-HCl, pH 8.8. The stacking gel contained 3.75% (w/v) acrylamide and 125 mM

Tris-HCl, pH 6.8. After separation, the gels were washed in 50 mM Tris-HCl, pH 7.0, and 5 mM $MgCl_2$ for 1 min and then incubated at 37 °C in a staining solution containing 50 mM Tris-HCl, pH 7.0, 5 mM $MgCl_2$, 5.3 mM Glc-1-P, 0.25 mM NADP, 0.25 mM NAD, 0.1 mM phenazine methosulfate, 0.25 mM nitroblue-tetrazolium, and 40 units of Glc-6-P dehydrogenase until PGM activity bands appeared.

### 3.3.3 Extraction of starch interacting proteins

#### 3.3.3.1 Extraction of proteins weakly interacting to starch

500 mg starch (split in five 2 mL Eppendorf tubes containing 100 mg each) were used for protein extraction. For the isolation of proteins weakly interacting to the starch surface (WIP), two washes with 200 µL 2% (w/v) SDS were performed per each 100 mg starch. The supernatant containing the WIP was recovered after vortex and centrifugation of samples during 10 min at 20 000 g. The collected supernatant was pooled in a single tube and further concentrated.

#### 3.3.3.2 Extraction of strong interacting proteins to starch

Following extraction of weak interacting proteins, starch samples were washed twice with 1 mL 4° C cold distilled water. Then, 1 mL of protein extraction buffer (0.2 M Tris-HCl, pH 6.8, 2% (w/v) SDS, 20% (w/v) glycerol, 50 mM DTE) (Helle et al., 2018) was added per each 100 mg starch, vortexed and boiled at 99 °C for 20 min. Afterwards, samples were centrifuged at 20 000 g for 10 min and the supernatant collected and further concentrated.

### 3.3.4 Concentration of protein samples

Supernatant containing the starch interacting proteins was transferred to a 10 kDa filter (Merck Millipore ®, 5 mL volume capacity) for protein concentration following the supplier manual instructions or into a 2 mL Eppendorf tube for acetone precipitation of proteins.
Proteins were precipitated with -20 °C cold acetone by adding 4 times the volume of the protein samples, vortexed and kept in -20 °C for at least 1 hour. Then, samples were centrifuged at 20 000 g for 5 min. The proteins were pelleted, and the acetone discarded. Tubes were left opened for 10 min to allow the samples to dry. Protein pellet was resuspended in 20- 40 µL of protein sample buffer (Helle et al., 2018).

### 3.3.5 Determination of protein concentration

Starch interacting protein samples were resuspended in 100 µL of protein extraction buffer to carry out the Bicinchoninic assay (BCA; Thermo Fisher Scientific, Waltham, MA, USA) following the manual instructions.

### 3.3.6 Electrophoretic separation of proteins

Starch interacting protein samples were separated through sodium dodecyl sulfate-polyacrylamide gel electrophoresis (SDS-PAGE) using different polyacrylamide concentrations varying from 7.5 to 10%. 30 µg protein was mixed with a 3X concentrated sample-denaturing buffer (0.5 M Tris-HCl pH 6.8, 180 mM DTE, 6% (w/v) SDS, 30% (v/v) glycerol, and 2% (w/v) bromophenol blue) in a 2:1 (v/v) proportion and heated at 90 °C for 5 minutes for protein denaturation. Electrophoresis was performed at 180 V and 40 mA.

### 3.3.7 Staining of SDS-PAGE gels

Following electrophoresis, protein bands were visualized by staining the gels overnight with a commercial Coomassie-blue staining solution (Roti Blue® - purchased from Roth, Germany) or by the silver staining procedure established by Shevchenko et al. (1996).

### 3.3.8 Quantitation of protein bands

Relative intensity of the protein bands detected by Coomassie-blue staining on SDS-PAGE gels was determined using the image processing program ImageJ (available for downloading on https://imagej.nih.gov/)

### 3.3.9 Mass spectrometry analysis

#### 3.3.9.1 Samples preparation

SDS-PAGE protein bands were prepared for mass spectrometry analysis following the protocol described by Webster et al. (2012) with some modifications. Bands were excised from the gel, cut into smaller pieces, and distained in 100 µL of 100 mM $NH_4HCO_3$/ 100% acetonitrile (1:1) during 15 mins with a change of distaining solution in between. Later, gel pieces were dehydrated in 50 µL acetonitrile during 5 min. The acetonitrile was discarded, and gel pieces were later dried in vacuum. Gel pieces were rehydrated with 15 µL of pre-cooled trypsin solution (20 – 30 ng/µL trypsin sequencing grade reconstituted in 50 mM

$NH_4HCO_3$) and left on ice during 15 min. 10 µL of 50 mM $NH_4HCO_3$ was added to cover the gel pieces and subsequently incubated overnight at 37 °C for trypsin digestion.

The extraction of tryptic peptides was performed according to the method described by Fettke et al. (2011). 20 µL distilled water was added to the samples and incubated for 15 min. The peptides were extracted out from the gel pieces by adding 20 µL acetonitrile and recovering the solution after 5 min. The same volume of 5 % (v/v) formic acid was added later to the gel pieces and incubated for 15 min. Finally, a second acetonitrile extraction was performed. The peptide extracts were pooled and completely dried in a vacuum concentrator. The pellet containing the peptides was resuspended in 10 µL of 20 % (v/v) acetonitrile dissolved in 0.1% (v/v) trifluoracetic acid (TFA).

#### 3.3.9.2 Protein identification

Trypsin-digested proteins were analyzed through mass spectrometry using a MALDI- TOF system (Microflex II RFT, Bruker, Bremen, Germany) and MS/MS MALDI-LTQ XL (Thermo Scientific). 0.35 µL peptide sample was spotted on the target plate and covered with the same volume of α-cyano-4-hydroxycinnamic acid (HCCA) matrix prepared as follow: 3.5 mg HCCA dissolved in 84 % (v/v) acetonitrile, 13 % (v/v) ethanol, and 3 % (v/v) distilled water. Peptide mass spectra (m/z 500 – 4 000 Da) were acquired as positive ions using the reflector mode. The peptide mass values were searched either against the Swissprot or NCBI databases listed in the Mascot Peptide Mass Fingerprint and Mascot MS/MS search platforms (http://matrixscience.com). Trypsin was selected as digesting enzyme and the peptide tolerance set to 0.5- 0.6 Da. One or no missed cleavage was allowed for the search and no fixed or variable modifications selected. For MS/MS ion search, the peptide charge was set to +1 and the MS/MS tolerance to 0.6 Da. Matches with a score above the threshold ($p < 0.05$) in the Mascot report were considered significant.

### 3.3.10 Western blot

The transfer of proteins from SDS gels to nitrocellulose membranes was carried out placing two Whatman filter papers, the membrane, the SDS-gel and two Whatman filter papers in a blotting device (Bio-Rad) following the manual instructions. All components were previously wetted with transfer buffer (25 mM Tris, pH 8.2; 192 mM glycine; 20 % MeOH (v/v). Blotting was performed overnight at room temperature at 12 V.

#### 3.3.10.1 Immunodetection of proteins

Blots were incubated for one hour in blocking TBST solution (100 mM Tris-HCl, pH 7.5, 150 mM NaCl, 0.1 % (w/v) Tween 20) containing 3% (w/v) milk powder and then with primary antibodies diluted 1:1000 (v/v) in blocking solution. After one hour, the primary antibody solution was removed and the membranes were washed during five minutes with TBST buffer (100 mM Tris-HCl pH 7.5, 150 mM NaCl, 0.1 % (v/v) Tween 20). This washing step was repeated six times. Later, blot membranes were incubated with secondary antibody (anti-mouse or anti-rabbit conjugated to alkaline phosphatase) or horseradish peroxidase (HRP) for one hour. The membranes were washed again with TBST buffer as mentioned. To visualize alkaline phosphatase activity, BCIP®/NBT (5-bromo-4-chloro-3-indolyl-phosphate/nitro blue tetrazolium) reagent (Sigma-Aldrich) was used following the manual instructions. For HRP conjugated antibodies, signal was detected using the Supersignal West Pico PLUS Chemiluminescent Substrate kit (Thermo Fisher) following the protocol described in the kit manual.

### 3.3.11 Analysis of soluble glucans in potato tuber discs following incubation with sugar and sugar-phosphates

#### 3.3.11.1 Incubation of potato tuber discs with Glc, Glc-6-P and Glc-1-P

Peeled potato tubers were sliced and cut in discs using a cork borer (8 mm diameter, c. 2 mm thick). Tuber discs were washed three times with 300 mL 4°C cold distilled water. Then, 1 g (10- 12 discs) was incubated per triplicate in Falcon tubes containing 20 mL of treatment solutions. All the experimental solutions were prepared with 50 mM citrate-NaOH (pH 6.5) as buffer, and were supplemented either with 10 mM Glc, 10 mM Glc-6-P or 10 mM Glc-1-P. In control solution, the sugars were omitted. Experimental incubation periods were 5-, 15-, 30-, 60-, and 120-min. Falcon tubes containing the tuber disc samples in the incubation solution were kept under agitation during the incubation time.

#### 3.3.11.2 Extraction of soluble glucans from tuber discs

After removing the treatment solutions, discs were frozen in liquid nitrogen and homogenized with an Ultra-Turrax for 20 sec in 3 mL of 20 % (v/v) cold ethanol. Following centrifugation (12,000 g, 10 min, 4 °C), the supernatant containing the soluble glucans was collected and heated (10 min, 99 °C). A centrifugation (20,000 g, 10 min) step was

performed to pellet the precipitated proteins. 1 mL supernatant was recovered and completely dried in a vacuum concentrator (Speedvac Savant SPD11V from Thermo ®) obtaining a pellet of carbohydrates.

### 3.3.11.3 Estimation of carbohydrates amount by reducing end assay

Amount of reducing sugars was estimated according to Waffenschmidt et al. (1987) using different concentrations of Glc as standard. For this, the carbohydrate pellet was resuspended in 100 µL distilled water. 2 – 5 µL of resuspended sample was mixed with 500 µL of 1:1 reacting solution (solution A + B, Table 1) and the volume completed to 1 mL with distilled water. Samples were incubated 15 min at 99 °C. Finally, samples were cooled down on ice and the OD measured at 560 nm.

**Table 1 Reacting solutions used for the estimation of reducing sugars amount**

Solution A

| | |
|---|---|
| 2,2´ Bichinchonine-4,4´dicarboxylic acid, disodium salt | 2.5 mM |
| Sodium carbonate | 256 mM |
| Sodium hydrogen carbonate | 144 mM |

Solution B

| | |
|---|---|
| Copper sulfate x 5 $H_2O$ | 2.5 mM |
| L- Serin | 6 mM |

### 3.3.11.4 Capillary electrophoresis with laser-induced fluorescence (CE-LIF)

100 nmol of reducing sugars were derivatized with 1 µmol 8-aminopyrene-1,3,6-trisulfonic acid, trisodium salt (APTS) dissolved in 2.0 µL of 1 M sodium cyanoborohydride in tetrahydrofuran and 1.5 µL of 1.2 M citric acid. The samples were incubated for 1.5 h at 55 °C and then diluted with 96 µL ultrapure water. Samples were diluted 5 times with ultrapure

water prior to injection in a Beckman Coulter PA800-plus Pharmaceutical Analysis System (Beckman Coulter, Brea, CA, USA) equipped with a silica capillary (inner diameter: 50 µm; outer diameter: 360 µm; length: 60 cm). The capillary was rinsed with separation buffer composed of 25 mM lithium acetate buffer (pH 4.75, adjusted with acetic acid) containing 0.4 % (w/v) polyethylene oxide.

The separation was performed at 30 kV during 20 min. The detection was made with a 488 nm solid-state laser module and a laser-induced fluorescence (LIF) detector.

#### 3.3.11.4.1 CE-LIF data analysis

##### 3.3.11.4.1.1 Degree of polymerization assignment

The degree of polymerization (DP) of the MOS samples was determined comparing the migration time of the peaks observed in the electropherograms against the migration time of standard samples prepared with 1 mg of maltotriose and maltohexaose (DP3 and DP6, respectively) and 1 mg of commercial maltodextrin (Sigma Aldrich) derivatized with APTS.

##### 3.3.11.4.1.2 Calculation of the relative amount of MOS

The area of every single MOS peak observed in the electropherogram was added up starting from maltotriose (DP3) up to the longer DP detected. Then, the area of each individual peak was divided by the total sum of areas and multiplied by 100, obtaining the relative amount (in percentage).

### 3.3.11.5 Statistical analysis

Three experimental units were used per incubation treatment. Three independent experiment repetitions were performed. Dunnett´s multiple comparison test against control incubation was performed for statistical analysis ($\alpha$=0.05). Additionally, analysis of variance ANOVA was used for multiple treatment comparison ($\alpha$=0.05).

# Part I

# Starch interacting proteins in potato tuber

# 4 Results

### 4.1 Starch interacting proteins profile

Proteins interacting with the starch granules were isolated from potato tuber starch, concentrated, and separated by SDS-PAGE. To elucidate the nature of the interaction within the starch granules, protein isolation was conducted in two steps. Weakly interacting proteins to starch (WIP), more likely located on the starch surface, were first recovered through successive washes with SDS. Later, strong interacting proteins (SIP) were recovered mixing the starch samples with protein extraction buffer while disrupting the granular structure through heat-induced gelatinization. In Figure 2, an initial assay using 100 mg of starch for protein isolation followed by SDS-PAGE separation is presented. In the separation gel stained with Coomassie-blue (Figure 2A, lanes 1-3), few protein bands were detected in the SIP fraction and a ~65 kDa band was predominant. In the WIP fraction (Figure 2A, lanes 4-6) only one band was visible. When the separation gel was silver stained following the method described by Shevchenko et al. (1996), notably more bands were visualized in both fractions (Figure 2B). In successive experiments, 500 mg starch was used for protein extraction, achieving this way a considerable increase in the protein amount recovered, reaching on average 30 µg for the SIP fraction and 8 µg for WIP. In Figure 2.1A, an SDS-polyacrylamide gel separation of the total amount of SIP recovered from 500 mg starch is presented. Several protein bands in the range of 35 to 250 kDa were detected using Coomassie-blue staining. All the observed bands were excised, trypsin digested, and analyzed with mass spectrometry. On the right side of Figure 2.1A, the name of the identified protein is described next to the corresponding band. Relative band intensity was estimated to quantify the ratio of each of the SIP that were characterized (Figure 2.1B).

By way of example on how an identification was conducted, mass spectrometry data generated from the gel band that proved to be the potato LESV protein is presented in Figures 2.2 and 2.3. The theoretical peptide mass values obtained by *in silico* trypsin-proteolysis of the potato LESV sequence (accession number in Spud DB: Soltu.DM.06G014960.1) were compared with the mass spectra generated from a band with an apparent mass of ~65 kDa

in the separation gel. Red color letters in the LESV protein sequence (Figure 2.2) show the peptide sequences that correspond to the matching mass values enlisted in Figure 2.2, covering 21% of the whole sequence. Amino acid sequence of the matching peptides was confirmed through tandem spectrometry searching the fragmentation pattern against the Mascot MS/MS database (Figure 2.3). As it can be observed in Figure 2.3, a significant match resulted for a "uncharacterized protein" in *S. tuberosum* L. having the same amino acid sequence expected for the corresponding LESV tryptic peptide.

All the SIP identified in this study corresponded with proteins related with the starch metabolism, resembling the results obtained by Helle et al. (2018) who first published an extensive analysis of the potato starch proteome. From the identified proteins, GBSS is clearly the most abundant protein in strong interaction to the starch granules, followed by SS2 (Figure 2.1A and B). Besides GBSS, additional starch synthases were found strongly interacting to starch: SS1, SS2 and SS3. Proteins implicated in starch degradation like GWD, PWD, and SEX4, were not removable from starch by SDS, but where only recovered after gelatinization of starch in protein extraction buffer, meaning that they remain strongly attached to the starch granules.

Plastidial glucan phosphorylase PHO1, in counterpart, was barely detected and was the least abundant, concurring with the results presented by another research group (Helle et al., 2018; 2019).

A summary of the starch interacting proteins that were identified in this work, divided in SIP or WIP, is presented in Table 2 and 3, respectively.

### 4.2 Weak interacting proteins to starch

WIP that were removable using 2% SDS are summarized in Table 3. Few proteins were recovered by SDS washes and mostly included protease inhibitors. Among these, multicystatin, kunitz-type and cysteine protease inhibitor were identified. Multicystatin, an 86 kDa endopeptidase with capabilities to inhibit cysteine proteases (Green et al., 2013) was consistently the predominant protein band in SDS-PAGE gels where WIP were separated. It has been stated that multicystatin is well distributed throughout tuber tissue (Rodis et al., 1984; Nissen et al., 2009; Green et al., 2013). Kunitz-type serine protease inhibitor and cysteine protease inhibitor, both having a mass of nearly 24 kDa, were reported containing a vacuolar signal peptide (Stiekema et al., 1988; Ishikawa et al., 1994). In addition, the cytosolic form of glucan phosphorylase, PHO2, was also found weakly interacting to the

starch granules. All the WIP had in common that they are not proteins expressed in plastid/amyloplast. Therefore, their interaction with starch might have occurred during the homogenization of tubers for starch isolation and purification.

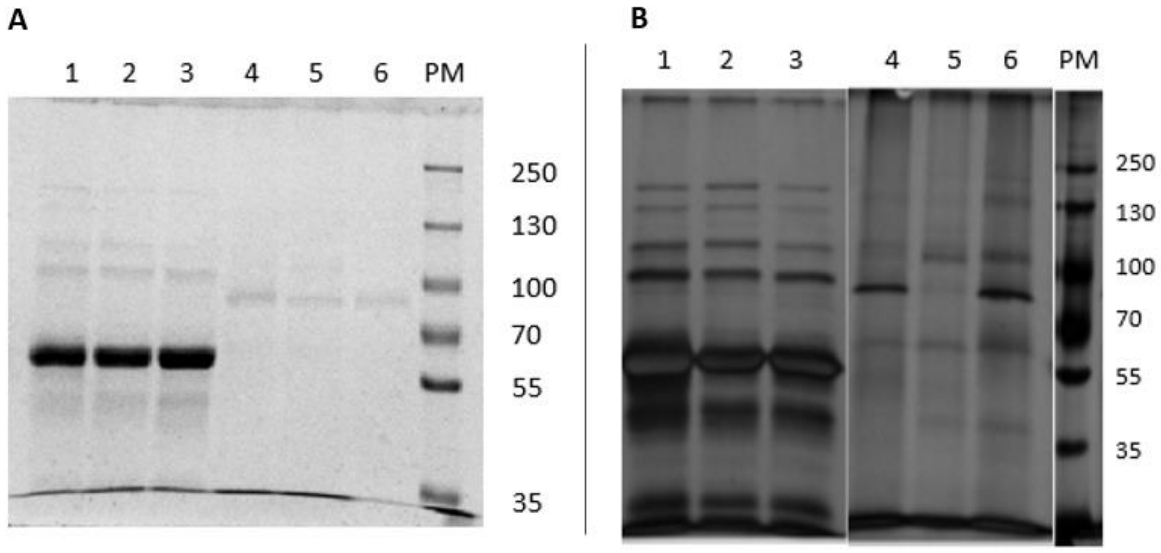


**Figure 2 7.5 % SDS-PAGE separation of starch interacting proteins in potato tuber**. In first attempts to isolate and characterize the starch interacting proteins, 100 mg tuber starch extracted from different potato lines was used. Protein extraction was performed in two steps to distinguish the weakly interacting proteins to starch (WIP) which were removable by SDS washes, from the stronger interacting proteins (SIP) which were recovered after gelatinization of starch in protein extraction buffer. Following extraction, protein samples were concentrated with Amicon® filters (10 kDa cutoff, 0.5 ml). Then, samples were separated in a 7.5 % SDS-PAGE. M: protein marker. In A, separation gel was stained with a Coomassie-blue solution (Roti ®-Blue from Carl Roth). In B, gel was silver stained (Shevchenko et al., l996). Lanes 1-3: SIP fraction. Lanes 4-6: WIP fraction. Lanes 1 and 4: Starch interacting proteins extracted from PGM-repressed line. Lanes 2 and 5: PHO1-repressed line. 3 and 6: Commercial potato var. Lilly.

**A**

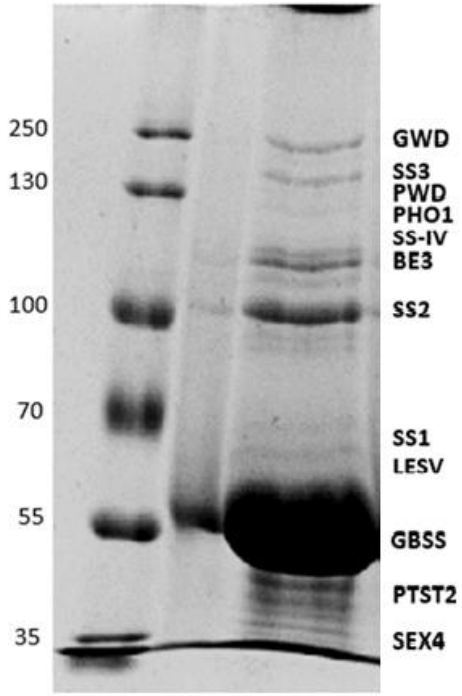


**B**

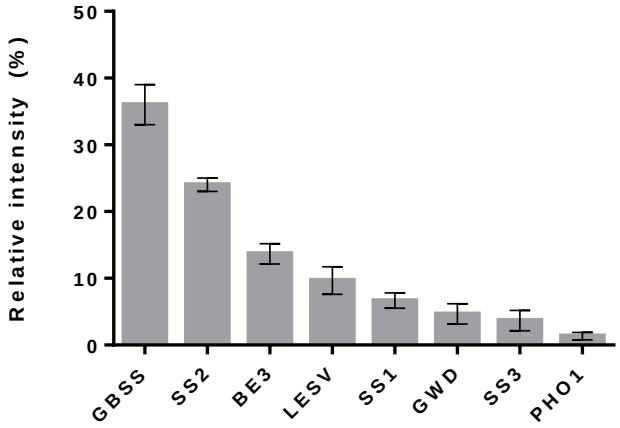


**Figure 2.1 7.5% SDS-PAGE separation of strong interacting proteins to starch. A.** Proteins strongly interacting to starch (SIP) in potato tuber were extracted from 500 mg starch. 30 µg SIP were separated in a 7.5 % SDS-PAGE. For visualization of the protein bands, the separation gel was stained with Roti ®-Blue (Carl Roth). **B.** Relative intensity of SIP bands in the separation gel was quantified using the image processor ImageJ. Three different gel images of SIP samples extracted from different starch batches were used for quantitation.

**Soltu.DM.06G014960.1**| LESV homologue protein. Mw: 63 447

```
         10         20         30         40         50         60
MATRFPATTH SRVVAASSGE PKVEYPFSVS TRKWQVVTER RRKNSRIKAT DSDSFLEMWK

         70         80         90        100        110        120
RAMERERKSA EFKRIAENIA PPEVEESPEI LEKKTEEFNK ILQVSPEERD KVQSMQIIDR

        130        140        150        160        170        180
AAAALAAAKA LIKENPLPRK DDDEADKNNK QGATGNVISI VPRSGTMMGT PGPSFWSWTP

        190        200        210        220        230        240
PSDSSFDDIQ MKSDVSLSPD PPSPVIEKER SPDFLSIPFQ SATIDRKHSP PLPPLQSHLE

        250        260        270        280        290        300
VENLEDSSST PEIPHQVEER ELGILFSANA AEAAYALHQE NEASSEGISP DGSRWWKETG

        310        320        330        340        350        360
TERRPDGVVC KWTLTRGISA DKTVEWEDKY WEAADEFGHK ELGSEKSGRD AAGNVWHEFW

        370        380        390        400        410        420
KESMWQSGGL VHMEKTADKW GRNNKGEEWH EKWWEHYGAG GQAEKWAHKW CSIDPNTPLD

        430        440        450        460        470        480
AGHAHVWHER WGEKYDGKGG SIKYTDKWAE RFEVDGWSKW GDKWDENFDL NGHGVKQGET

        490        500        510        520        530        540
WWAGKHGERW NRTWGEGHNG SGWVHKYGKS SDGEHWDTHV NEETWYERFP HFGFFHCFQN

        550
SVQLREVKRP SDWP
```

Sequence coverage: 21.8%

**Theoretical Mw (monoisotopic mass): 63447.69**

| Mass | Position | Peptide Sequence |
|---|---|---|
| 3727.8197 | 228-260 | HSPPLPPLQSHLEVENLEDSSSTPEIPHQVEER |
| 3504.6513 | 261-294 | ELGILFSANAAEAAYALHQENEASSEGISPDGSR |
| 2376.9752 | 510-528 | SSDGEHWDTHVNEETWYER |
| 1793.9068 | 211-226 | SPDFLSIPFQSATIDR |
| 1551.7087 | 493-506 | TWGEGHNGSGWVHK |

**Figure 2.2 LESV identification through peptide mass fingerprint analysis.** A protein band with an apparent mass of ~65 kDa was cut out from the separation gel, trypsin digested, and analyzed through MALDI-TOF. Sequence of the homologue Arabidopsis LESV protein in potato with the accession number "Soltu.DM.06G014960.1", annotated in Spud DB is given. In red are the peptide sequences of the spectra masses matching with the theoretical masses of *in-silico* trypsin digestion of potato LESV sequence.

**Peptide View**

MS/MS Fragmentation of **SPDFLSIPFQSATIDR**
Found in **XP_006350655.1** in **NCBIprot**, PREDICTED: uncharacterized protein LOC102584633 [Solanum tuberosum]

Match to Query 1: 1793.492724 from(1794.500000,1+) scans(0) rtinseconds(0)
Title: controllerType=0 controllerNumber=1 scan=1
Data file 12-1794_G12-qb.mzML

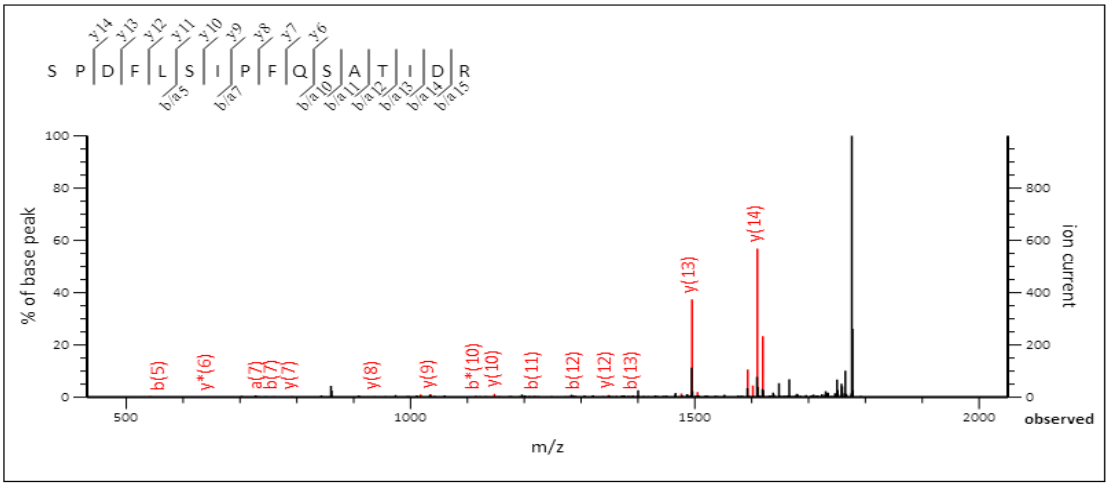


**Figure 2.3 MS/MS identification of LESV peptide.** Peptide masses matching with the potato LESV predicted tryptic peptides were analyzed through tandem spectrometry. After searching in MS/MS Mascot database the fragmentation pattern of the ion with a parental mass of 1793.49 Da, the peptide sequence corresponded with a potato LESV peptide.

**Table 2 Identification of potato proteins strongly interacting to starch**

| Protein Name | Accession num. (Uniprot/Spud DB) | Predicted MW (Da) | Seq. Cov. (%) | Score | Identification Method | Cell location |
|---|---|---|---|---|---|---|
| **GWD** | Q9AWA5 | 163 136 | 12 | 105 | MALDI-TOF | Chloroplast |
| **SS3** | Q43846 | 139 024 | 18 | 80 | MALDI-TOF | Chloroplast |
| **PWD** | D2JRZ6 | 132 277 | | N.A. | Immunodetected | Chloroplast |
| **PHO1** | P04045 | 109 400 | 1 | 29 | MS/MS | Chloroplast |
| **BE3** | P30924 | 99 021 | 9 | 116 | MS/MS | Chloroplast |
| **SS2** | Q43847 | 85 168 | 27 | 159 | MALDI-TOF | Chloroplast |
| **SS1** | P93568 | 70 608 | 13 | 80 | MS/MS | Chloroplast |
| **GBSS** | Q00775 | 66 576 | 24 | 138 | MALDI-TOF | Chloroplast |
| **LESV** | Soltu.DM.06G014960.1 | 63 400 | 21 | 77 | MS/MS | Chloroplast |
| **PTST2** | XP_006367350 | 47 255 | | N.A. | Immunodetected | Chloroplast |
| **SEX4** | Soltu.DM.11G004900.2 | 41 569 | | N.A. | Immunodetected | Chloroplast |

**Table 3 Identification of weak interacting proteins to starch**

| Protein Name | Accession Number | Predicted MW (Da) | Seq. Cov. (%) | Score | Identification Method | Cell location |
|---|---|---|---|---|---|---|
| **PHO2** | P32811 | 95 052 | 23 | 108 | MALDI-TOF | Cytosol |
| **LOX 13**<br>**Probable linoleate 9S-11 oxygenate** | Q43189 | 96 974 | 11 | | MALDI-TOF | Cytosol |
| **Multicystatin** | P37842 | 86 731 | 16 | | MALDI-TOF | N.D. |
| **Probable inactive patatin 3-Kuras PT3** | Q3YJS9 | 41 117 | 8 | | MS/MS | Vacuole |
| **Kunitz type protease inhibitor** | AAB32802.1 | 24 500 | | 51 | MS/MS | Vacuole |
| **Cysteine protease inhibitor 10** | O24383 | 20 962 | 37 | | MALDI-TOF | Vacuole |
| **Cysteine protease inhibitor 8** | O24384 | 24 694 | 31 | | MALDI-TOF | Vacuole |

### 4.3 Starch interacting proteins in transgenic lines

To evaluate if changes in the profile of the starch interacting proteins could be observed, two transgenic potato lines were selected for starch isolation, both sustaining a deficiency in the same catalytic activity but in different cell compartments, and we compared it with the starch interacting proteins in wild type tubers. Thus, a transgenic line repressing the glucan phosphorylase PHO1 isozyme, which is expressed in the amyloplast/chloroplast, and a second line repressing the cytosolic phosphorylase PHO2 was used. The PHO1 is directly involved in starch and maltodextrin metabolism (Fettke et al., 2010; Castellanos et al., 2022), whereas PHO2 is involved in starch degradation related maltose metabolism in the cytosol (Fettke et al., 2005). Repression of the targeted enzymes in the transgenic lines was confirmed through Native-PAGE separation of buffer-soluble proteins and subsequent detection of phosphorylase activity (Figure 2.4). In Figure 2.5, starch interacting proteins extracted from the three lines and separated in SDS-PAGE gel is presented. The protein profile obtained from the transgenic lines and wild type was comparable, with no substantial differences either on the WIP or SIP.

However, on the WIP fraction obtained from wild type starch, a clear band with an apparent mass of 100 kDa was observed, which was not visible in the same fraction of the transgenic lines (Figure 2.5A, See WIP fraction). This band was excised and further identified through mass spectrometry as the cytosolic PHO2. Thus, as a contaminating protein. In potato tuber starch with antisense inhibition of PHO2, the corresponding band was not visible.

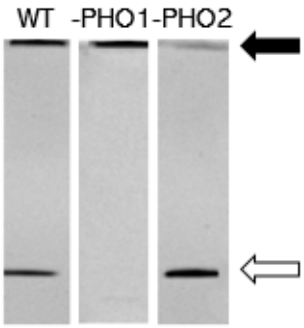


**Figure 2.4 Native-PAGE separation of buffer-soluble proteins.** Soluble proteins were extracted from potato wild type tubers, and two transgenic tubers repressing the plastidial (PHO1) and cytosolic (PHO2) phosphorylase enzyme. The procedure used for phosphorylase activity detection was described by Castellanos et al. (2022). On each lane, 20 µg buffer-soluble protein was loaded. The separation gel contained 0.2% (w⁄ v) glycogen. Black arrow indicates the position of PHO2; white arrow, PHO1.

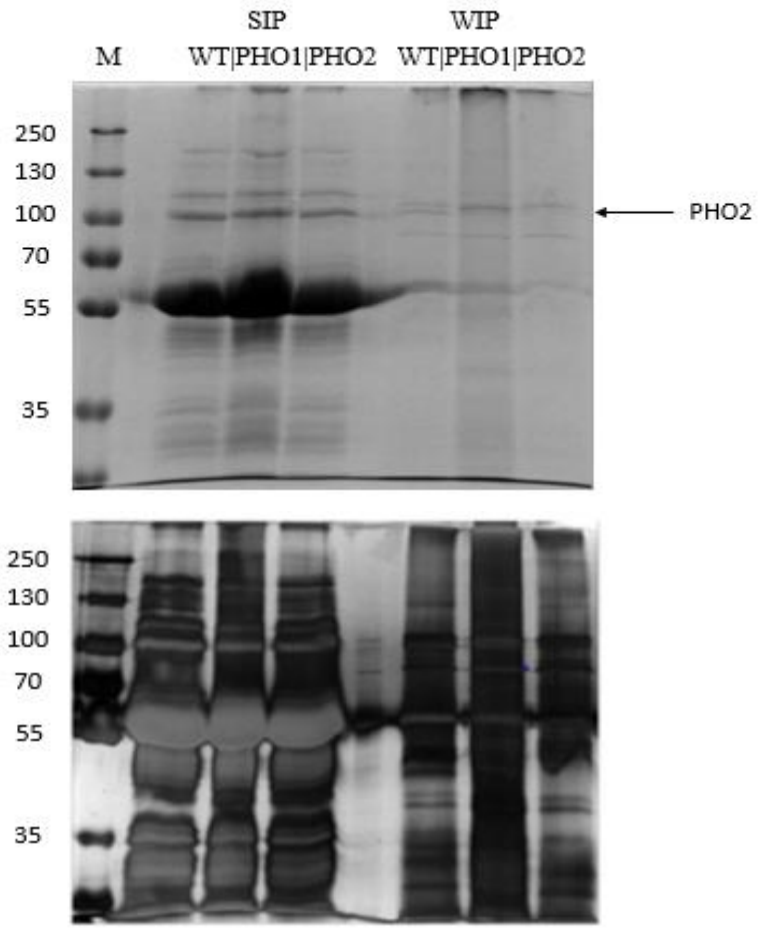


**Figure 2.5 9.5 % SDS-PAGE of starch-interacting proteins isolated from wild type, PHO1-repressed and PHO2-repressed transgenic tubers.** Starch interacting proteins isolated from 500 mg starch were separated in a 9.5% SDS-PAGE. Gel was stained with Rotiblue® (Carl Roth) (A) or silver stained (B). A band with an apparent mass of 100 kDa was observed in the protein fraction of wild type weakly interacting to starch (WIP), which corresponded to the cytosolic PHO2.

Similarly, in PHO1-repressed lines this additional band was not observed. However, the background of the stronger contamination of the starch with PHO2 is obscure but can be related to surface properties of the isolated starches. In this regard, it was already shown that various mutants related to starch metabolism showed different starch granule surface properties (Mahlow et al., 2014).

In addition, we detected the proteins bound to starch with antibodies raised against specific enzymes involved in starch degradation (GWD and PWD) or initiation (PTST2) using the three different genotypes. GWD and PWD were not removable from starch by SDS washes and were exclusively found as SIP (Figure 2.6). PTST2, as it was expected for its role in starch initiation, was found in the SIP fraction. Similarly, an antibody against PHO1 was also utilized (Figure 2.6). However, as previously indicated, the detected band corresponded to the cytosolic isoform PHO2, which was strongly detected in the WIP fraction.

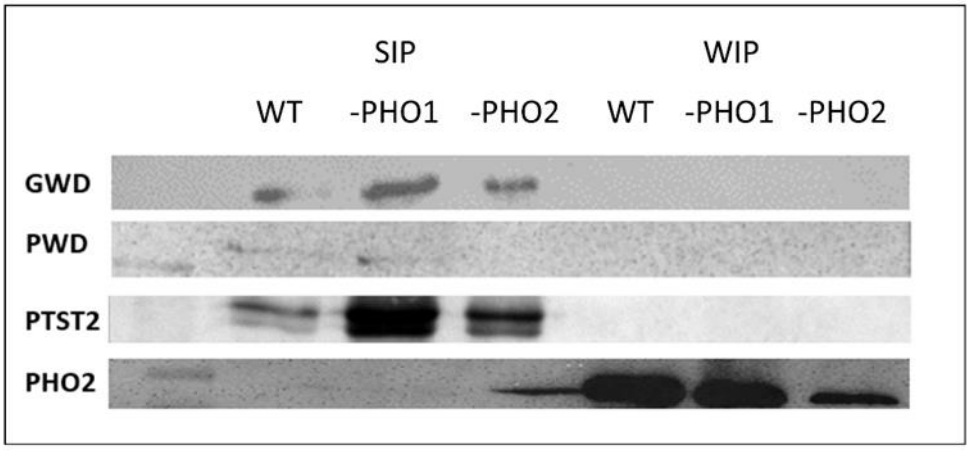


**Figure 2.6 Immunodetection of proteins interacting to potato starch.** Starch interacting proteins isolated from wild type, PHO1-repressed, and PHO2-repressed potato tubers were separated in a 9% SDS-PAGE and transferred to a nitrocellulose membrane for western-blot. Specific antibodies for A. thaliana GWD, PWD, PTST2 an PHO1 were used for immunodetection. GWD, PWD and PTST2 were detected as SIP. Using an antibody specific for the AtPHO1, a nearly 100 kDa protein was detected in the WIP fraction. However, through mass spectrometry analysis, it turned out that it corresponded to the cytosolic PHO2 isoform.

### 4.4 Changes in the protein band pattern of WIP to starch was distinguished when tubers were stored under different conditions

As shown, PHO1 was detected as SIP, but not as WIP. Considering previous indications that PHO1 plays an active role on the starch metabolism in potato and rice plants growing at low temperatures (Orawetz et al., 2016; Hwang et al., 2016), the isolation of the starch interacting proteins was assayed after storage of wild type and PHO1-repressed tubers under different temperatures. Right after harvested, tubers derived from the same plant were stored at room temperature, warm (37 °C) or cold (4 °C) conditions for 15 days in the dark, and starch interacting proteins were later extracted. In the SIP fraction, no differences on the protein band pattern were observed. However, as it can be observed in the SDS-PAGE gel image of WIP (Figure 2.7), disparities on the detection of protein bands were evident comparing the wild type samples against PHO1-repressed samples, and even on the same genotype stored under different conditions. For instance, a nearly 55 kDa protein band was observed in the PHO1-repressed tuber stored at room temperature and faintly at 37 °C, but not at 4 °C. Whereas, in wild type samples the same protein band was missing in the three cases. More notably, a protein band having a mass close to 130 kDa was detected on the WIP only in PHO1-repressed tuber stored at 4 °C (Figure 2.7). Thus, it seems that the WIP protein pattern was altered among the various conditions, which requires further clarifications.

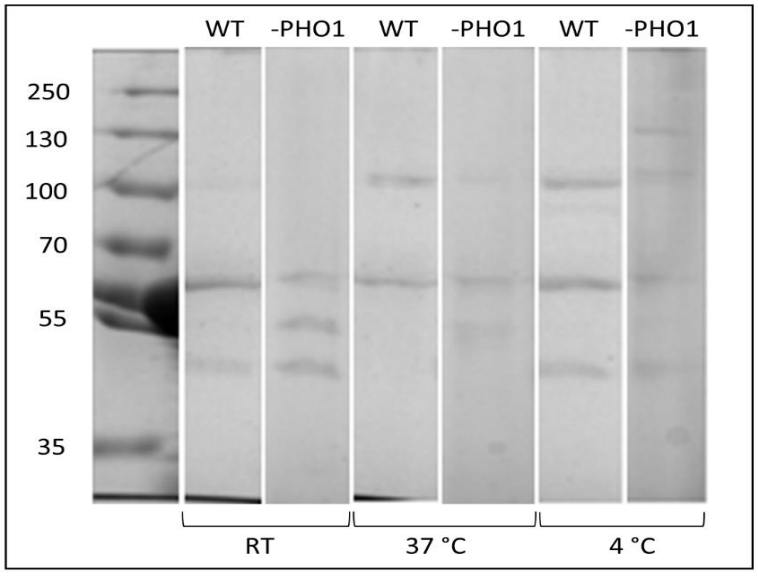


**Figure 2.7 7.5 % SDS-PAGE separation of weak interacting proteins to starch in wild type and PHO1-repressed tubers.** Immediately after harvested, wild type and PHO1-repressed tubers were stored 15 days at room temperature, warm (37 °C) or cold (4 °C) conditions. WIP were isolated with 2% (w/v) SDS and separated by electrophoresis in a 7.5% polyacrylamide gel.

# 5 Discussion

## 5.1 Proteins were mainly contained in the SIP fraction

The starch interacting proteins in potato starch were explored under different conditions. We classified the starch proteins in two different fractions based on the nature of the interaction, considering the way we isolated them from starch. One fraction contained the proteins that were removable from starch by SDS and thus, more likely found loosely interacting with the starch surface, defined here as weak interacting proteins (WIP). Strong interacting protein fraction (SIP) was designated to the proteins which were able to recover only after breaking down the granular structure of the starch by heat-induce gelatinization. All identified proteins from the SIP were described as involved in starch metabolism. The protein profile of the SIP observed in the separation gel mainly resembles that obtained by Helle et al. (2018). GBSS was the most profuse protein, followed by SS2. The least abundant SIPs were PWD and PHO1. Interestingly, in case of GWD and PWD, which are dikinases mainly involved in starch degradation, it would be assumed that they might act on the starch surface based on the catalytic function they realize. However, no traces of neither of both phosphotransferases were recovered through consecutive washes of starch samples with SDS. Thereby, both enzymes remained closely interacting within the starch granules.

Finding these phosphorylating dikinases strongly interacting with potato starch is not surprising, as it was previously demonstrated that phosphorylation occurs along the whole storage starch biosynthesis and accumulation in potato tubers (Nielsen et al., 1994). However, the exact role that phosphorylation might play during synthesis of starch has not been precisely described but it is in focus of interest. Besides their role in starch degradation, probably for additional processes like, for instance, during the arrangement of the starch structure, the activity of these enzymes might be necessary but not totally indispensable, since the tuber yield and tuber starch content in transgenic plants repressing GWD was not compromised (Lorberth et al., 1998). This assumption would be especially applicable in this case, where mainly accumulation of starch takes place in developing tubers. Thus, finding enzymes strictly and only linked to starch degradation would not be expected.

Regarding the WIP proteins, the amount of protein that was possible to isolate from starch was considerably lower than the recovered from the SIP fraction (around 8 μg against ~30 μg of SIP), and less protein bands were detected after gel electrophoresis and staining. From the seven WIP that were identified, five corresponded to protease inhibitors. It is believed

that protease inhibitors in plants are storage proteins that act as defense mechanism in cases of wounding-respond and represent around 50% of the total soluble proteins in potato tubers (Pouvreau et al., 2001; 2003). Considering this data, the fact that starch proteases were found interacting to starch is not surprising. On the other hand, as these proteins are not expressed in plastids, where starch is accumulated in plants, we assume that the interaction of the protease inhibitors with the starch granules must have occurred during the starch purification procedure from tubers rather than naturally occur under physiological conditions. The same assumption can be followed for the cytosolic phosphorylase PHO2 which was also found in the WIP fraction. It is well known that PHO2 possesses a strong affinity towards branched glucans, like starch´s amylopectin (Fettke et al., 2004; 2005). Therefore, the chance to find PHO2 attached to the starch granules after homogenizing of tuber tissue would be very likely.

### 5.2 PHO1 is not a starch granule-bound protein

As we were able to detect only very small amount of PHO1 through MS/MS analysis in SIP but not in WIP, even though PHO1 was found expressed in significant amounts after extraction of total proteins from potato tuber (Jørgensen et al., 2006), we assayed the detection and location of the plastidial PHO1 in the two protein fractions using an antibody raised specific against the homologue protein in *A. thaliana.* Proteins were isolated from potato wild type starch and transgenic PHO1-repressed and PHO2-repressed potato starch samples. A 100 kDa protein band was detected in the starch surface protein fraction (Figure 2.8A). However, after PMF analysis and data search against the Mascot protein database, a significant match turned out for the cytosolic PHO2, which has 95 kDa size. The fact that a reduced immunodetection signal was observed in the starch bound protein sample obtained from potato with strong repression of PHO2 was in accordance with the results (Figure 2.8A). A possible interaction of the anti-*At*PHO1 with *St*PHO2 epitopes could not be excluded since both, the plastidial and cytosolic potato phosphorylase protein sequences share highly conserved regions (see Figure 2.8B). On the other hand, since PHO2 is expressed in the cytosol and possess strong affinity towards branched glucans like starch´s amylopectin, it can be assumed that its localization within the starch is more related with protein contamination during the starch isolation procedure rather than being a starch-associated protein.

In case of PHO1, failing to detect it within the WIP indicates that, although this enzyme is fundamental in the carbohydrate and starch metabolism, in potato tuber starch it does not remain attached to the granules. This observation is supported by Tetlow et al. (2020) who stated that the plastidial phosphorylase (SP, PHS1 or PHO1) and disproportionating enzyme 1 (DPE1), though localized in the plastid stroma, are in general not granule-associated enzymes. This characteristic would be consistent with the function that both enzymes have modulating and supplying soluble substrates for other enzymes (Tetlow et al., 2020).

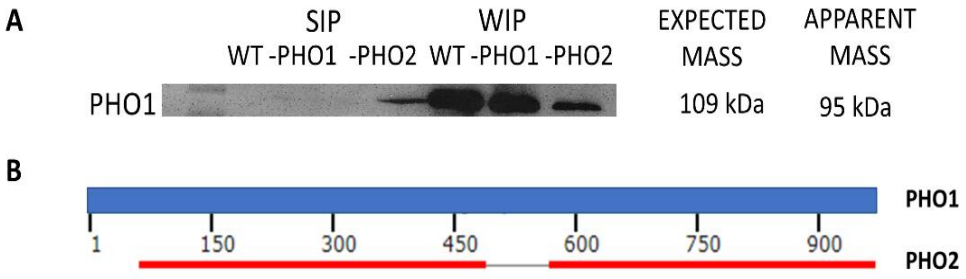


**Figure 2.8 PHO immunodetection in potato starch bound proteins. A.** Starch bound proteins separated by SDS-PAGE were transferred to a membrane for immunoblotting and detection using a plastidial phosphorylase (*At*PHO1) specific antibody. A nearly 95 kDa size protein band was detected in the starch-surface proteins of wild type and the two transgenic lines with PHO1 and PHO2 antisense inhibition. Through PMF analysis, the corresponding band was identified as the *S. tuberosum* cytosolic phosphorylase isoform PHO2. **B**. Protein BLAST alignment of *S. tuberosum* PHO1 and PHO2 shows two highly conserved regions among the two sequences. The first region comprises the amino acid 62 - 487 in PHO1 sequence, and the second region from 566 - 965.

### 5.3 Effects of genotypes and storing conditions on proteins bound to starch granules

After identification of the proteins that were regularly found interacting with starch, the question arose whether differences could be traceable on the starch proteome in potato plants containing alterations in enzymes that are closely linked to the carbohydrate metabolism. To investigate this possibility, we used a transgenic potato line with strong repression of the plastidial glucan phosphorylase activity and another repressing the same activity but in the cytosol. However, no obvious differences were observed after SDS-PAGE separation of the SIP and WIP extracted from PHO1-repressed, PHO2- repressed and wild type tubers. In wild type and the two transgenic potato lines, we also assayed the detection of starch interacting proteins using specific antibodies. GWD and PWD were found in the SIP fraction in the three different potato starch samples. Protein targeting to starch 2 (PTST2), a chloroplastic protein involved in starch granule initiation (Seung et al., 2017), was also immunodetected in the three different genotypes as SIP having a 43.3 kDa mass.

On a second approach seeking for differences on the starch interacting proteins, we stored PHO1- repressed and wild type tubers under different temperature conditions. By this mean, different patterns of WIP protein bands were visualized between the samples stored at room temperature, 4 °C or 37 °C, either in wild type or PHO1-repressed tubers. Differences were basically observed in the loss/detection of four bands having an apparent mass of ~ 130, ~100, ~50 and ~45 kDa. Unfortunately, due to the low protein concentration of these bands, attempts to identify them were so far unsuccessful. Noteworthy, a nearly 130 kDa protein was detected in the PHO1-repressed protein sample obtained from potato tubers stored at 4 °C, which is close to the molecular weight of PWD. Under such cold storing conditions, the storage starch is more likely under the so called cold-induced sweetening phenomenon, thus degradation of starch must occur in order to self-supply reducing sugars. In any case, this band was not detected in wild type tubers stored at 4 °C and a relationship to be attributed to the missing PHO1 activity in the transgenic tuber triggering the expression of PWD is hard to establish.

Considering the findings presented by Feike et al. (2016) who reported the presence of ESV1 in both the soluble and insoluble (starch-containing) protein fractions in *A. thaliana* and *N. sylvestris*, and Helle et al. (2018), who recently reported the identification of ESV1 (48.9 kDa) in the starch-associated proteins of potato tuber, we consider the probability that one of the WIP bands we observed might correspond to this protein.

Attempts to further investigate the starch proteome under variable environments or simulated stress conditions would be supportive in revealing inducing mechanisms for specific starch-related enzymes and understanding their implication under specific conditions. Like we observed in this assay, expression of different starch interacting proteins was stimulated by storage of tubers in different temperatures.

# Part II

# Maltodextrin analysis in potato tuber samples

# 6 Results

## 6.1 The MOS metabolism of wild-type tubers was significantly affected by incubation with glucose-1-phosphate

We first evaluated whether parenchyma cells from freshly harvested wild-type potato tubers incubated with Glc and Glc-6-P during 30- and 60-min revealed an altered maltooligosaccharide content. The relative amounts, expressed as a percentage of each degree of polymerization from the total MOS detected by CE- LIF, are depicted in Figure 3. MOS with up to DP10 were detected following Glc-6-P incubation as well as in controls. However, following Glc-6-P incubation, an increase in the relative amount of maltotriose (DP3) and maltohexaose (DP6) was observed in both incubation times. This was accompanied with a decreased proportion of maltotetraose (DP4) and maltopentaose (DP5), more remarkable after 60-min. In samples incubated with glucose, MOS with a maximal DP7 were detected together with a significant increase in the amount of DP3, whereas all other DPs revealed no alteration or reduced amounts.

In another series of incubation experiments including a solution containing an equal amount of Glc-1-P (Figure 3.1), longer MOS up to DP30 were detected. Comparing the various DPs, a drop in the relative amounts of DP3 to 5 was noticed following Glc-1-P incubation compared to Glc-6-P, Glc, and control. Most likely, these shorter glucans were elongated and formed the observed extended MOS. Further, following the incubation with Glc-1-P, a significant increase in the total amount of MOS was detected (Figure 3.2), whereas for Glc-6-P and glucose incubation no alteration was observed compared to control.

## 6.2 The plastidial phosphorylase was responsible for the longer and higher amounts of MOS following glucose-1-phosphate incubation

Following incubation with Glc-1-P, we observed more and longer MOS. As Glc-1-P is the substrate used for phosphorylases, we tested whether the reduction in the phosphorylase activities would have an influence on the observed alteration of the MOS metabolism. As it was shown that Glc-1-P was taken up by the parenchyma cells and directly transported into

the amyloplasts (Fettke et al. 2010, 2011), we included both isoforms in our analysis. Therefore, we incubated Glc-1-P with transgenic tuber discs repressing either the plastidial or cytosolic glucan phosphorylase (Figure 3.3; see also Fettke et al. 2011) and wild-type discs for 60 and 120 min (Figure 3.4). For each genotype, the difference between the relative

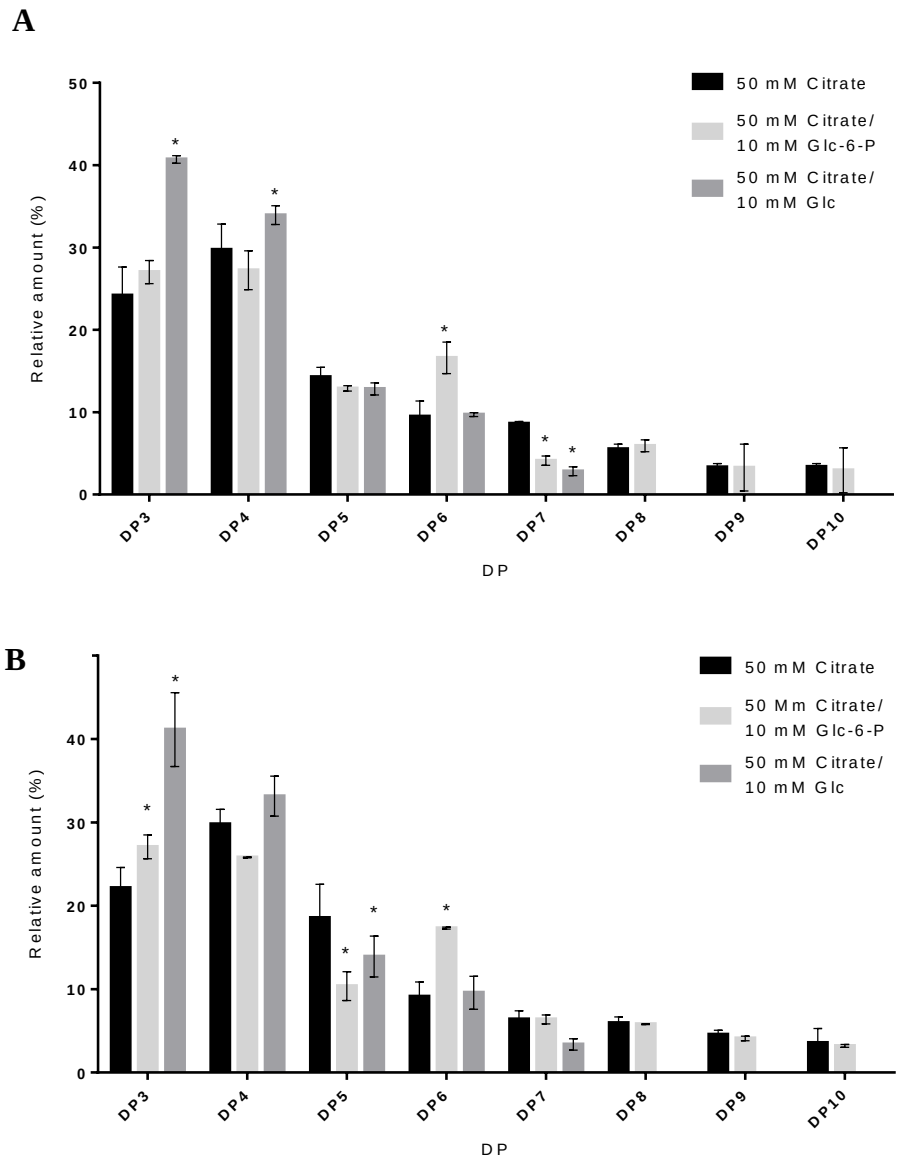


**Figure 3 Maltodextrins in potato tubers following incubation with various sugars and sugar derivatives.** Relative amount (%) of MOS in potato wild type tuber discs after 30- (**A**) and 60 min (**B**) incubation in 50 mM citrate (control solution) and two treatment solutions, one supplemented with 10 mM Glc-6-P and the second with 10 mM Glc. The effect of Glc and Glc-6-P in the MOS metabolism was evaluated by incubating discs from freshly harvested wild type tubers in the mentioned solutions. After incubation, soluble glucans were extracted in 20 % (v/v) ethanol, concentrated, and analyzed by CE-LIF. The mean of three biological replicas with standard deviation is presented. Dunnett´s multiple comparison test against control was used for statistical analysis ($\alpha$=0.05).

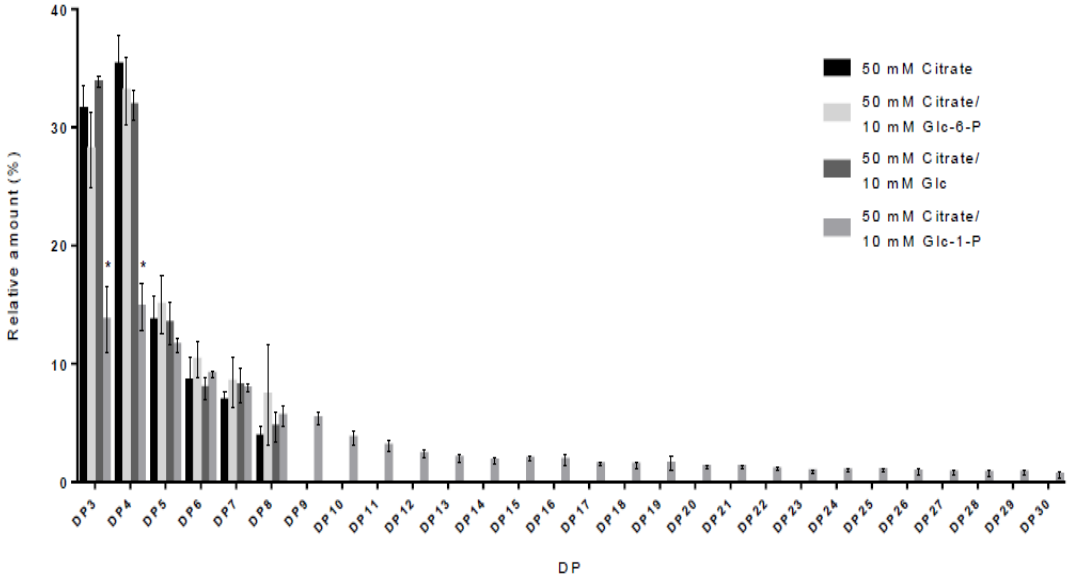


**Figure 3.1 Maltodextrins content in potato tubers following incubation with Glc-6-P, Glc, and Glc-1-P.** Relative amount (%) of MOS in potato wild type tuber discs after 60 min incubation in 50 mM citrate (control solution), Glc-6-P, Glc and Glc-1-P. In a second incubation experiment, where a treatment solution supplemented with Glc-1-P was included, an extensive proportion of MOS with higher degree of polymerization (up to 30) was detected. The mean of three biological replicas with standard deviation is presented. Two-way ANOVA was used for statistical analysis (α=0.05).

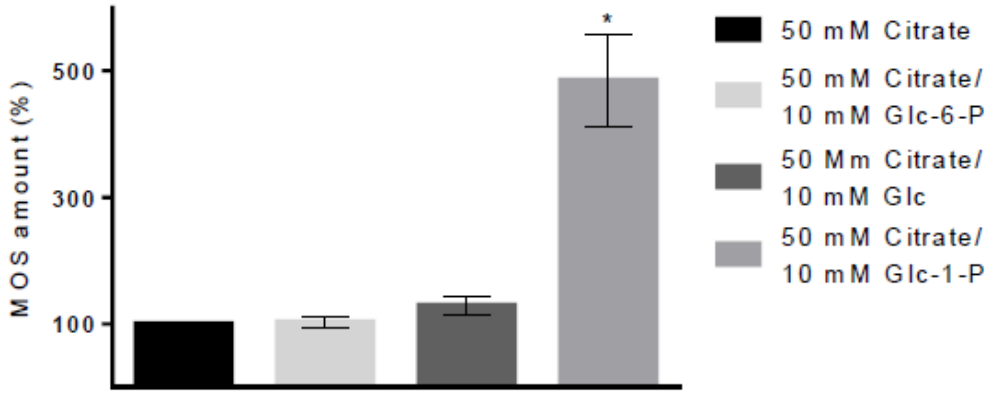


**Figure 3.2 Total amount of MOS detected by CE-LIF in wild type potato tuber discs after 60 min incubation in 50 mM citrate (control solution), Glc-6-P, Glc and Glc-1-P**. The mean of the total MOS amount obtained following incubation in control solution was set as 100 %. Thus, the increase amount in treatment solutions was calculated with respect to control. The mean of three biological replicas with standard deviation is presented. One way ANOVA was used for multiple comparisons (α=0.05).

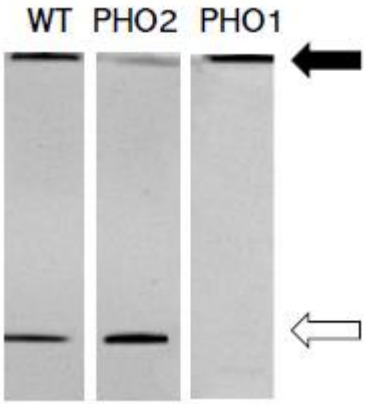


**Figure 3.3 Phosphorylase activity detection in native PAGE gel**. Buffer-soluble proteins were extracted from potato wild type, plastidial (PHO1) and cytosolic (PHO2) phosphorylase repressing tubers**.** In each lane, 20 µg protein was loaded. The separation gel contained 0.2% (w⁄v) glycogen. Following electrophoresis, the separation gel was equilibrated in 100 mM citrate-NaOH (pH 6.5) at room temperature for 10 min and then incubated for 30 min in a 100 mM citrate-NaOH (pH 6.5) plus 20 mM Glc-1-P solution. Subsequently, the separation gel was washed with water and latter stained with a solution containing 0.23 % (w/v) of KI (potassium iodide) and 0.13 % (w/v) $I_2$ (iodine) (Fettke et al., 2010). Black arrow indicates the position of cytosolic PHO2; white arrow, plastidial PHO1.

amount of MOS for each DP following incubation with Glc-1-P and the controls, where hexose phosphates were omitted, was graphed as difference, and expressed in percentage.
In PHO1-repressed tuber discs, almost null variation was observed in the MOS, except DP5, where an increase was seen in both incubation times (Figure 3.4). Nevertheless, unlike wild-type tubers, this transgenic line already contained maltodextrins with a higher degree of polymerization irrespectively of Glc-1-P incubation (Figure 3.5). PHO2 repression, in contrast, did not affect the capability of the tuber cells to form longer MOS, as a similar distribution of MOS to wild type was observed (Figure 3.4). Alterations were detected mainly for short glucan chains (DP3-DP6). Further, a longer incubation for 120 min revealed a very similar MOS pattern, pointing to a nearly saturated MOS metabolism (Figure 3.4B).
In another series of incubation experiments, discs from sprouting tubers that were stored for three months after harvested were used. As seen in Figure 3.6, for PHO1-repressed discs, again nearly no differences were estimated for each DP, meaning that incubation with Glc-1-P didn´t affect the MOS pattern in this genotype. In wild-type and PHO2-repressed tuber discs, a very similar proportion of glucans with a DP between 12 and 30 resulted after 30 and 60 min Glc-1-P incubation. For shorter MOS, a reduced amount was observed again in

the PHO2-repressed tuber discs (Figure 3.6). This data indicates that the utilization of the externally supplied Glc-1-P by the plastidial phosphorylase for MOS elongation was conducted regardless of the physiological state of the potato tubers.

In addition, besides PHO2-repressed tubers discs not being affected in the MOS formation capability, they consistently showed an even higher activity of the PHO1 isoform (Figure 3.3). Based on these observations, it was suggested that the decrease in shorter MOS was related to the rapid elongation and thus to a stronger shift of the MOS distribution for longer MOS during the same incubation time. Therefore, experiments with wild-type and PHO2-repressed tuber discs incubated with Glc-1-P for shorter periods were conducted (Figure 3.7). Following 5 min incubation, an extensive MOS generation was detected in both lines, showing that the Glc-1-P uptake and the generation of MOS is a fast process. Significant differences between wild-type and PHO2-repressed samples were observed in the relative proportion of DP3, DP4 DP6, DP9, and DP10 (Figure 3.7A). In PHO2-repressed sample, a lower percentage of DP6 and higher proportion of DP9 and 10 were observed compared to wild-type (Figure 3.7A). The total amount of MOS generated during Glc-1-P incubation was significantly higher in PHO2 compared to wild-type in incubation periods ranging from 5-30 min (Figure 3.7B).

Moreover, in tuber discs repressing PHO2, the MOS content increased more rapidly comparing the different incubation times (Figure 3.7B). All these observations were likely a consequence of the observed higher activity of PHO1 in tubers with antisense inhibition of PHO2, as compared to the wild-type control (see Figure 3.3).

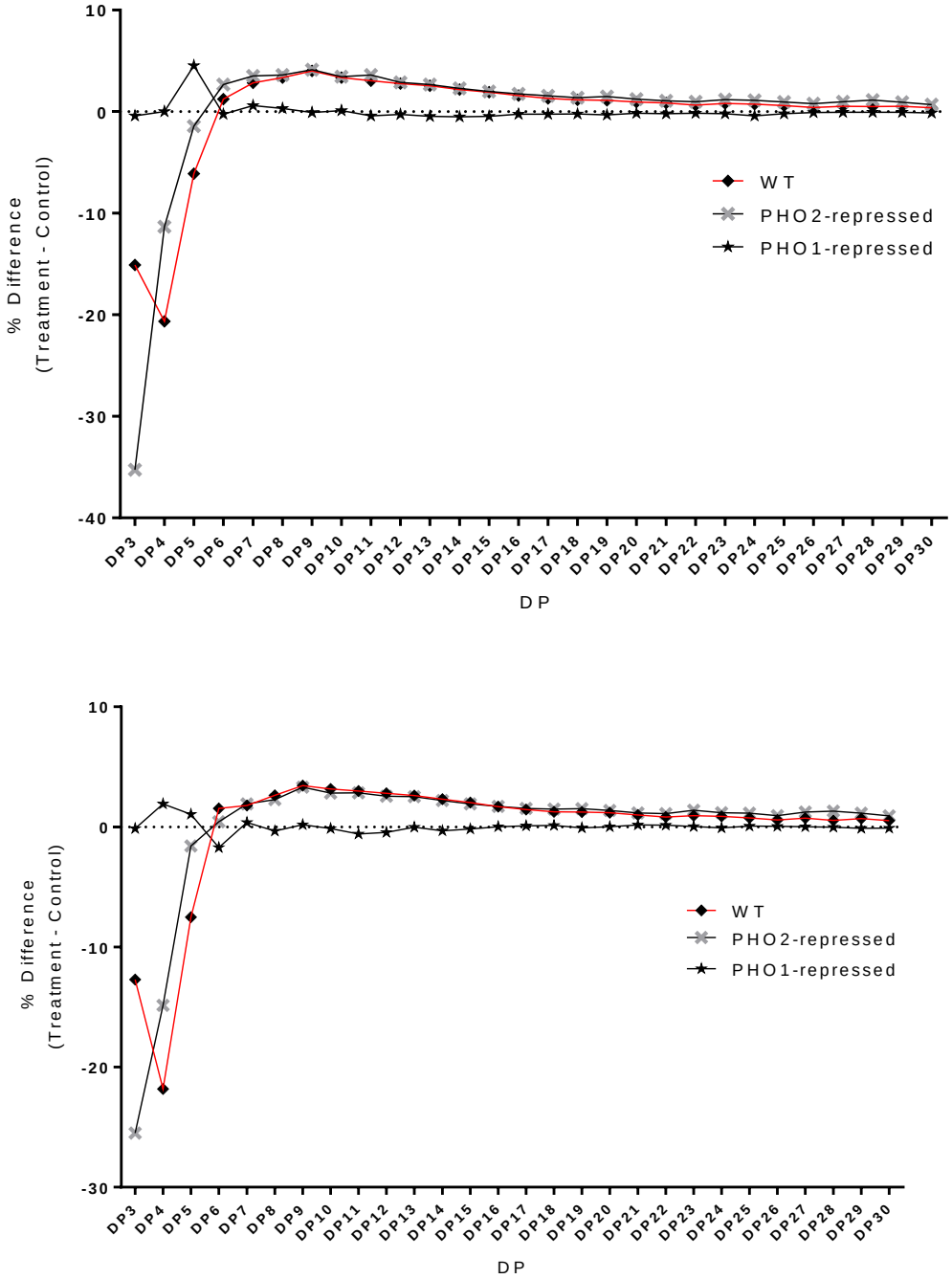


**Figure 3.4 MOS difference comparison between wild type tuber discs and potato lines repressing the cytosolic (PHO2) and the plastidial (PHO1) phosphorylase after 60- and 120-min incubation in control and 10 mM Glc-1-P solution**. Freshly harvested tuber discs from each line were used. Through CE-LIF analysis, the relative amount (%) of MOS was estimated and the difference for each DP in treatment minus control incubation was calculated and graphed as difference (%). Values are the difference between the means of three biological replicates used for treatment and control incubation

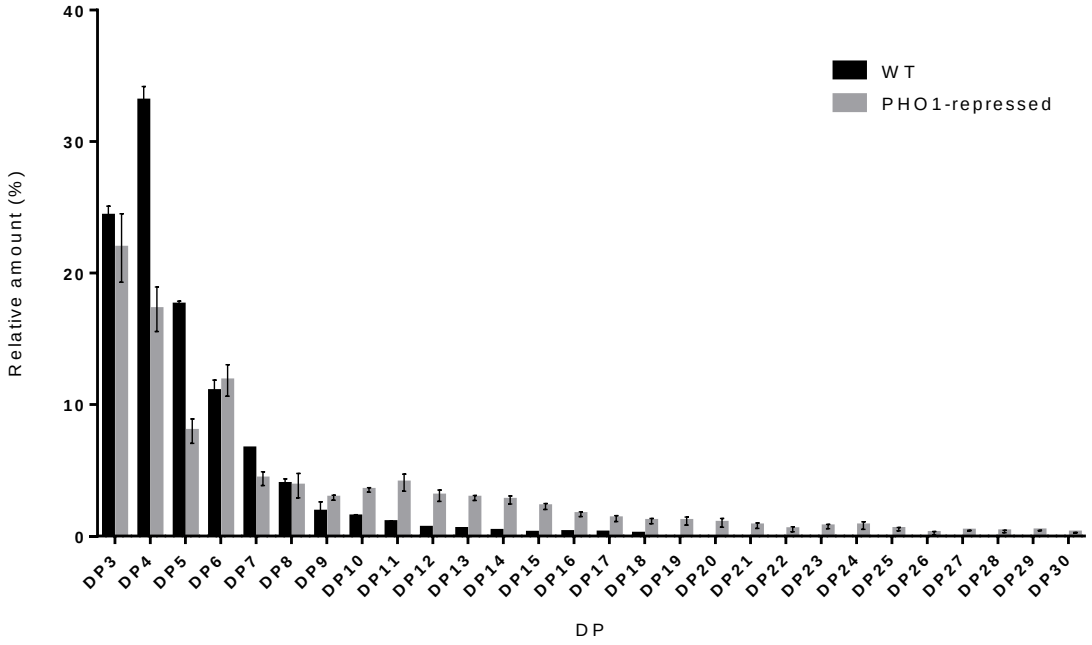


**Figure 3.5 Relative amount of MOS in wild type and PHO1-repressed tuber discs incubated in control solution.** WT and PHO1-repressing tubers were incubated 60 min in a control solution lacking hexose phosphate**.** The numbers are based on triplicates with bars representing the standard deviation.

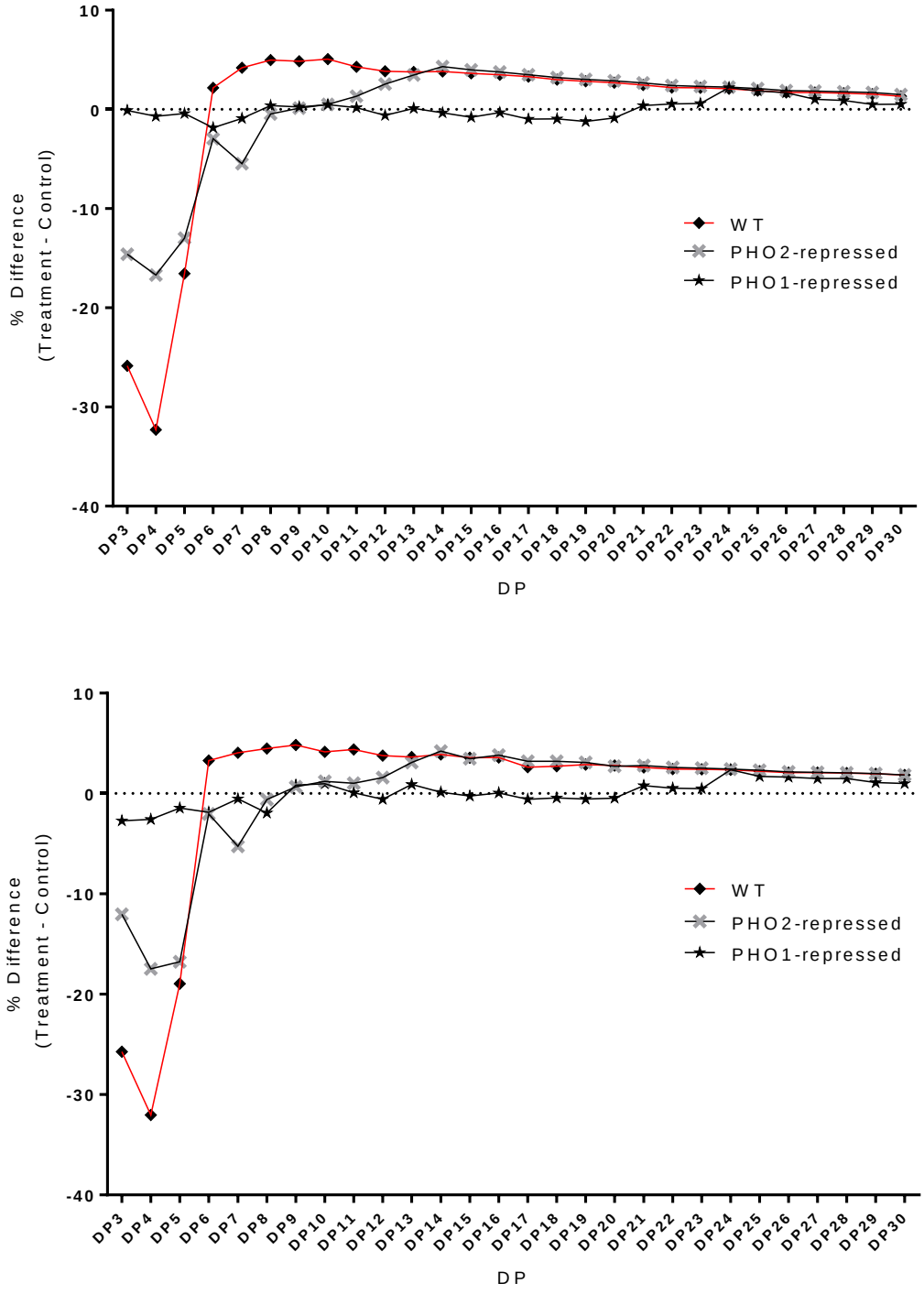


**Figure 3.6 MOS difference comparison in tuber discs from sprouting tubers.** Tuber discs from wild type, PHO2- and PHO1-repressed tubers that were stored for 3 months after harvested and showing sprouts were used for 30- and 60-min incubation in control and Glc-1-P solution. Values are the difference between the means of three biological replicates used for treatment and control incubation.

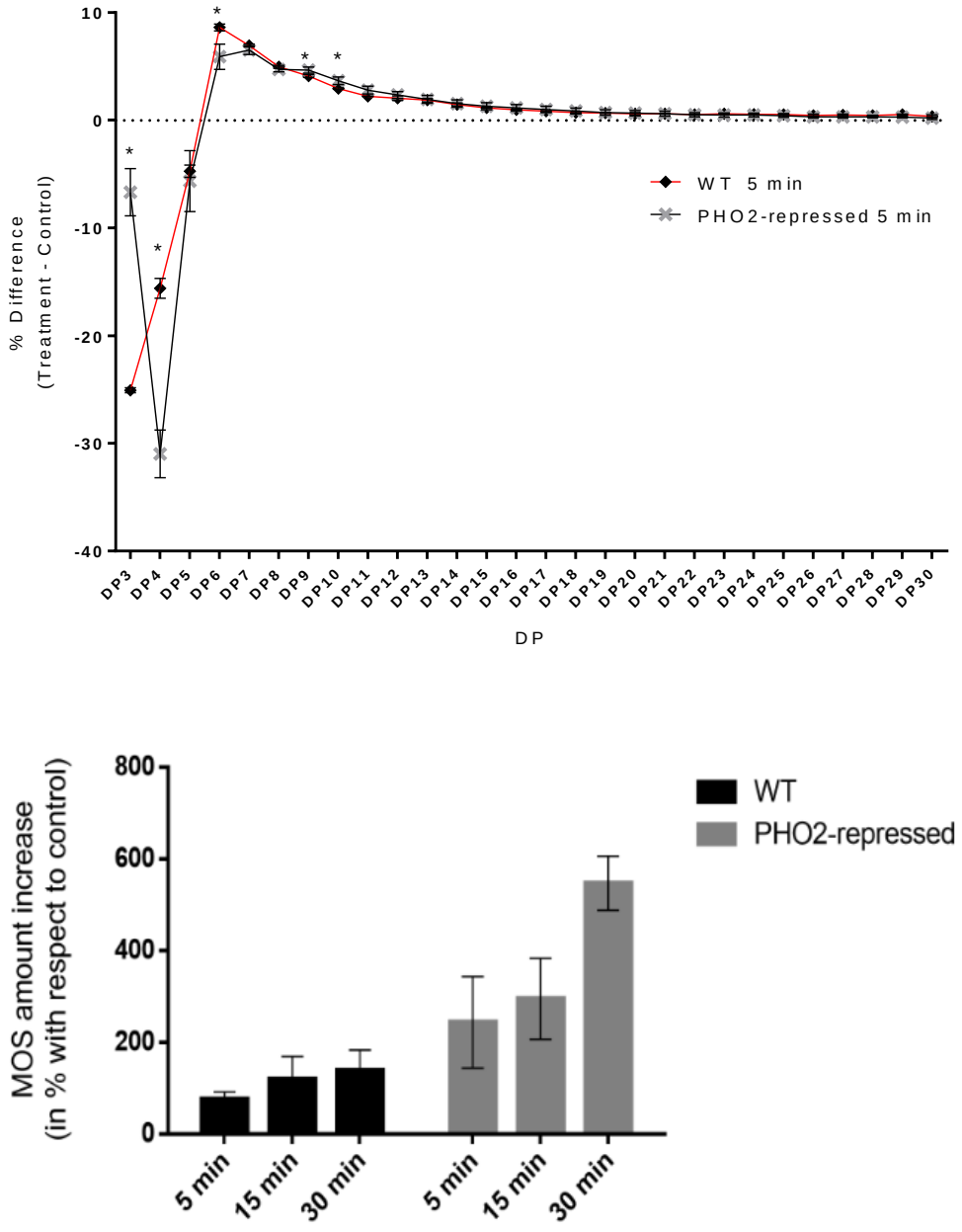


**Figure 3.7 Comparison of the maltodextrins from wild type and PHO2-repressed tuber. A.** MOS amount difference in wild type and PHO2-repressed tuber discs after 5 min incubation in control and Glc-1-P solution. For each genotype, 1 g (10 -12 potato tuber discs) tuber discs were incubated during 5 min in control solution with no hexose phosphate and treatment solution containing Glc-1-P. Relative MOS amount (given in percentage) was evaluated by CE-LIF. The difference of the relative MOS amount obtained after treatment minus control solution for each genotype is depicted. The numbers are based on triplicates. Bars represent standard deviations. Multiple T-test was used for statistical analysis ($\alpha$=0.05). **B.** MOS amount increase (%) in wild type and PHO2-repressed tuber discs after Glc-1-P incubation. The total amount of MOS detected by CE-LIF after control incubation was used to determine the increase proportion of MOS following Glc-1-P incubation with respect to control.

### 6.3 Phosphoglucomutase had no impact on the usage of Glc-1-P for MOS metabolism

Since the phosphoglucomutase (PGM) catalyzes the interconversion of Glc-1-P and Glc-6-P, we used a transgenic potato line simultaneously repressing the cytosolic and plastidial PGM activity to investigate whether a reduced turnover of the acquired Glc-1-P in the parenchyma cells would have an impact on the MOS formation. The antisense inhibition of PGM was followed via native PAGE and activity staining (Figure 3.8). The transgenic line revealed a strong reduction in the overall phosphoglucomutase activity (Figure 3.8; see also Fettke et al. 2008). Following 5-min Glc-1-P incubation of PGM-repressed and wild type tuber discs, the PGM-repressed line revealed a MOS pattern similar to the wild-type controls. However, a closer look revealed a lower amount in MOS with DP7–DP9 compared to wild-type (Figure 3.9). Despite revealing similar proportions of the MOS distribution after Glc-1-P incubation, determination of the percentage that the MOS amount increased after Glc-1-P incubation for 5-, 15- and 30-min with respect to control was conducted (Figure 3.10). In PGM-repressed discs the increasing amounts of MOS were significantly higher in the three incubation times compared to wild type (Figure 3.10). This data suggested that a more extensive utilization of Glc-1-P was enabled in PGM-repressed sample

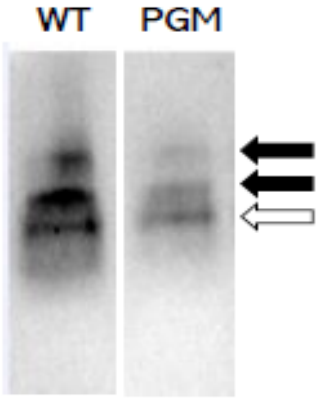


**Figure 3.8 Phosphoglucomutase activity detection in native PAGE gel.** Separation of buffer-soluble proteins extracted from potato wild type and transgenic tuber with antisense inhibition of both cytosolic and plastidial phosphoglucomutase (PGM) (Lytovchenko et al., 2002). PGM activity was detected following the procedure described by Egli et al. (2010). Black arrows indicate the position of cytosolic PGM; white arrow, plastidial PGM.

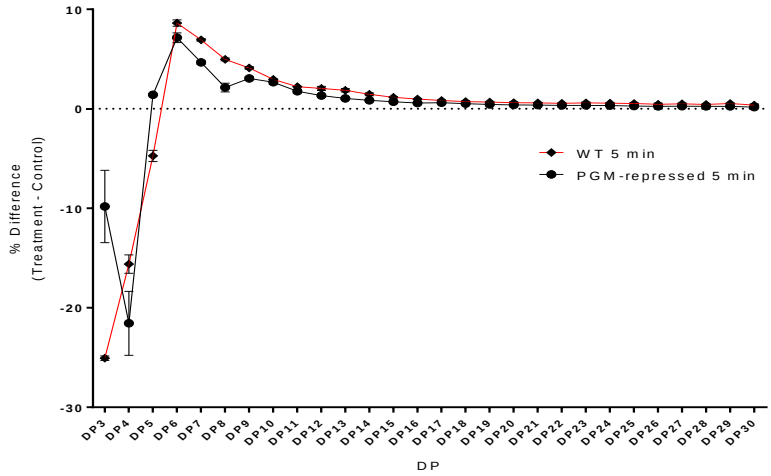


**Figure 3.9 MOS amount difference in wild type and PGM-repressed tuber discs after 5-min incubation in control and Glc-1-P solution.** Wild type and PGM-repressed tuber discs were incubated in Glc-1-P and control solution before extraction and analysis of MOS. The relative amount of MOS in Glc-1-P incubated samples minus control incubation is presented. Values are the difference between the means of three biological replicates used for treatment and control incubation.

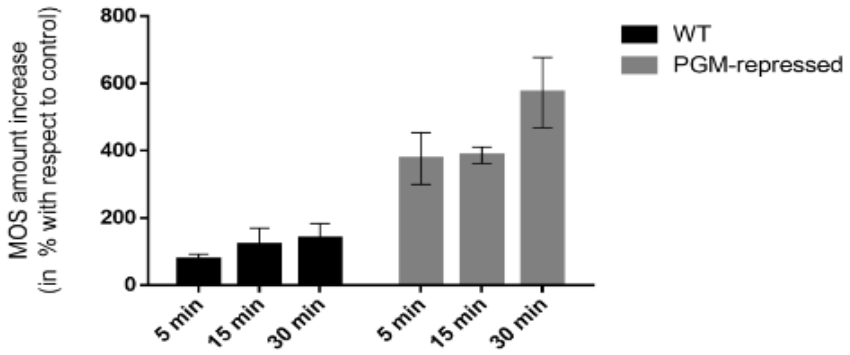


**Figure 3.10 MOS amount increase (in %) in wild type and PGM-repressing tuber discs after incubation with Glc-1-P with respect to control incubation**. The total amount of MOS detected by CE-LIF after control incubation was used to determine the increase proportion of MOS following Glc-1-P incubation with respect to control.

In the next step, we compared the total MOS amount in all the evaluated genotypes following Glc-1-P incubation. In the PGM-repressed line, the MOS content increased 34.6% compared to its control based on the estimation of reducing sugar amount (Table 4). Such an increase was considerably higher in comparison with wild-type, PHO2-repressed, and PHO1-repressed lines (11, 8 and 0 %), respectively. Regarding the intrinsic MOS content in all lines, thus the MOS without any incubation, PGM-repressed contained the highest MOS amount, followed by PHO1-repressed (Figure 3.11). In wild-type and PHO2-repressed line, the MOS content showed no significant difference and were the lowest. The relative MOS amounts in each of the evaluated lines after incubation in control solution is presented in Figure 3.12. As it is noticed, the PHO1-repressed line is the only one showing a very distinct pattern compared to wild type, characterized for containing much longer MOS in considerable proportions.

Overall, the experiments clearly showed that the uptake of Glc-1-P was directly used by PHO1 impacting on the MOS metabolism, and no detectable amount was transferred into Glc-6-P, which could, therefore, reduce the availability of Glc-1-P. Therefore, a linear utilization of Glc-1-P was demonstrated, including the uptake of Glc-1-P into the apoplasts and the direct metabolism via the plastidial phosphorylase into MOS metabolism.

**Table 4. MOS increase after 30 min incubation in Glc-1-P (in %).** For each genotype, the increase in the MOS amounts following incubation of tuber discs with Glc-1-P with respect to control samples was estimated using the reducing sugars assay.

| Potato Line | MOS increase following Glc-1-P incubation (%) |
|---|---|
| **WT** | **11 ± 1.5** |
| **PHO1-repressed** | **0 ± 2** |
| **PHO2-repressed** | **8 ± 1.7** |
| **PGM-repressed** | **34.6 ± 8.6** |

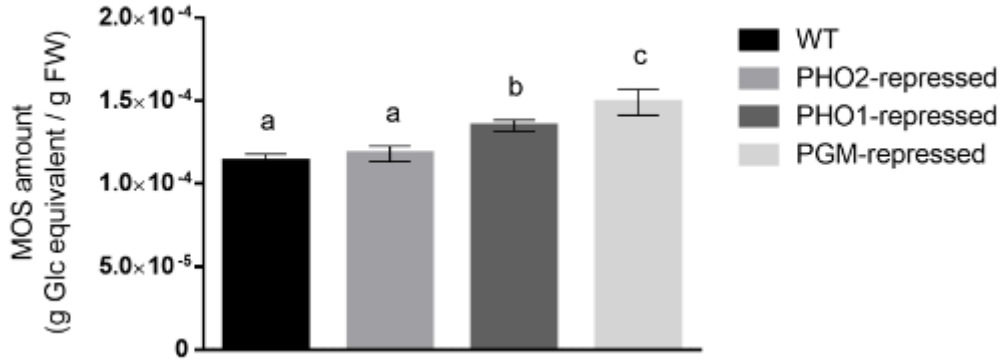


**Figure 3.11 MOS amount in wild type and transgenic PHO1-, PHO2-, and PGM-repressed tubers**. The MOS content (equivalent to grams of Glc per grams of fresh weight) was estimated based on the procedure established by Waffenschmidt et al. (1987) for reducing sugar amount determination using Glc as standard. The mean of three replicates with standard deviation is depicted. One way ANOVA was used for multiple comparisons (α=0.05). Different letters represent significant difference.

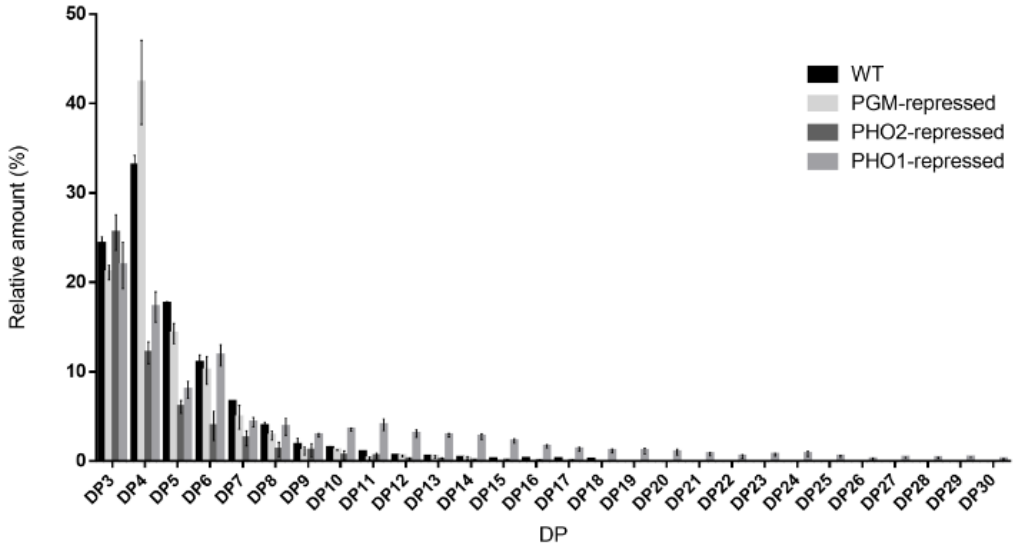


**Figure 3.12 Relative amount of MOS in wild type and transgenic lines repressing PGM, PHO2 and PHO1 following incubation in control solution**. Tuber discs samples from the different lines were incubated 60 min in 50 mM citrate (pH 6.5). As observed, in PHO1 repressing tubers, MOS with a degree of polymerization up to 30 (DP30) are detected after CE-LIF analysis.

### 6.4 DP5 was remarkably increased in green potato tubers

To analyze the MOS profile in green potatoes, thus performing photosynthetic activity, tubers from wild type and PHO1-repressed growing plants were exposed to light for 15 days by unearthing them from the $10^{th}$ week of plant growth until harvested ($12^{th}$ week). After harvested, greenish tubers were kept one additional week exposed to light in a growing chamber. As control samples, tubers from the same plants were kept covered up with soil during the entire plant growth until harvested. Control tubers were stored one week in the dark before extraction and analysis of MOS. As observed in Figure 3.13A, in wild type tubers exposed to light a higher proportion of MOS with DP5 was observed, together with a significant drop in MOS DP6 compared to wild type control tubers. A slight although significant decrease in DP4 proportion in comparison to control tubers was also noticed. Interestingly, in green tubers repressing PHO1 the same effect was observed (Figure 3.13B). DP5 was found considerably increased compared to control tubers. Relative amounts of MOS with DP7, 8 and 10 were also inferiors in green PHO1 tubers compared to control.

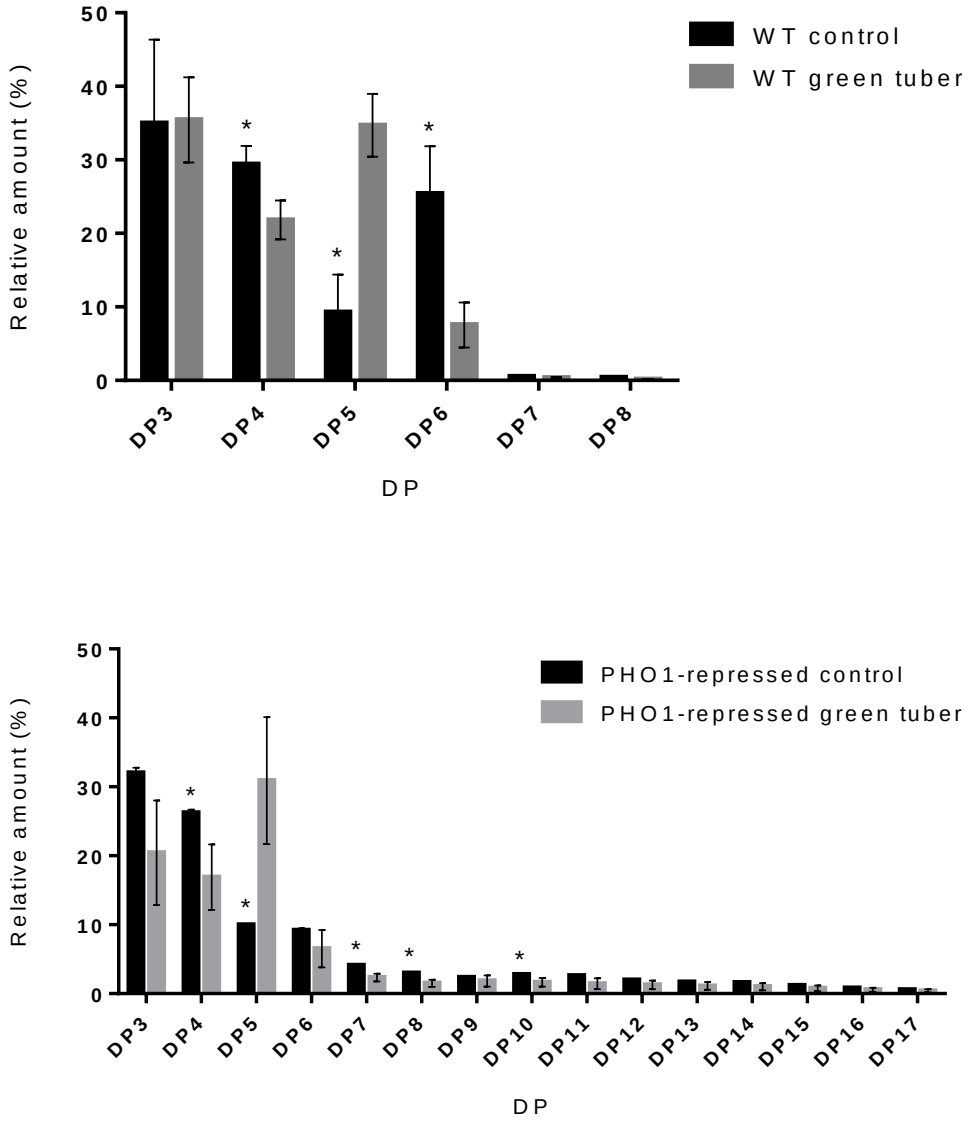


**Figure 3.13 Relative MOS amount in WT and PHO1-repressed green tubers exposed to light.** Growing tubers from wild type and transgenic PHO1-repressed potato plants were exposed to light from the 10th week of plant growth until harvested (12$^{th}$ week). Greenish tubers were kept one additional week exposed to light in a grow chamber. As control samples, tubers from the same plants were kept covered up with soil during the entire plant growth until harvested. After harvested, control tubers were kept one week in the dark before MOS extraction and analysis. As observed in **A**, WT tubers exposed to light showed a higher proportion of MOS with DP5, together with a significant drop in MOS with DP6 compared to control tubers. A slight although significant decrease in DP4 proportion compared to control tubers was also noticed. **B**. In PHO1-repressed green tubers also a remarkable increased of MOS DP5 is noticed, while decreasing the proportions of DP4 and 6 in comparison with control tubers without photosynthetic activity. Relative amounts of MOS with DP7, 8 and 10 were also inferiors in green PHO1 tubers compared to control.

# 7 Discussion

## 7.1 MOS metabolism of parenchyma cells was specifically and significantly altered following Glc-1-P uptake

Despite the relevance of MOS as constituents for starch formation and as degradation products, little focus has been placed on understanding their distribution, regulation, and implications. Previous studies already demonstrated that potato tuber discs and purified amyloplasts could utilize Glc-1-P more efficiently compared to other externally supplied sugars or sugar derivatives (such as glucose, sucrose, maltose, or Glc-6-P) (Naeem et al., 1997; Fettke et al., 2005; 2012), but the flux of the carbon source was monitored only towards starch. With the use of CE-LIF analysis of MOS isolated from potato tuber discs samples, we confirmed that Glc-1-P was more efficiently taken up into the parenchyma cells than glucose or Glc-6-P, and further incorporated into MOS. Glc-1-P revealed a significant effect on MOS metabolism that became evident in the increased amount of MOS following incubation and the massively altered chain length distribution (Figure 3.1 and 3.2). Even though a limited incorporation into starch have been found using $^{14}C$ labelled glucose and Glc-6-P (Naeem et al., 1997; Fettke et al., 2010), the incubation with these metabolites had no conspicuous effect. Therefore, we concluded that the MOS metabolism might be in some way either restricted to Glc-1-P or that in the normal parenchyma cell system, regulation mechanisms for high Glc-1-P levels are not well established. The latter seems to be a more plausible explanation considering that the Glc-1-P levels under normal conditions in the potato tuber cells are much lower than glucose or Glc-6-P (Tauberger et al., 2000; Lytovchenko et al., 2002; Fernie et al., 2002) and we used relatively high amounts of Glc-1-P. Despite the missing data regarding the concentration of Glc-1-P in the cell following the uptake, it is highly likely that this was considerably increased. If we consider that the Glc-1-P content in potato wild type developing tubers is around 12 nmol per gram of fresh weight (Tauberger et al., 2000; Fernie et al., 2002), we can then estimate that quantities in the order of 21.1 to 28.6 nmol of Glc-1-P were incorporated and used in the formation of the longer MOS following 5- and 30-min incubation, respectively.

Further, a significant turn-over of Glc-6-P into Glc-1-P and vice versa was excluded; otherwise, a similar alteration of MOS metabolism would be expected following incubation of tuber discs with Glc-6-P. In this regard, the thermodynamic equilibrium of the conversion of the glucose phosphates is on the side of Glc-6-P (Atkinson et al., 1961; Tewari et al.,

1988) and therefore, it is expected that at least a portion of Glc-1-P is converted to Glc-6-P. That specific effect of Glc-1-P was observed on the MOS metabolism and further indicated that a high amount of Glc-1-P entered the cells.

## 7.2 MOS were localized in the amyloplast, and their metabolism was affected by PHO1

We tested the capability of PHO1-repressed and PHO2-repressed potato tubers, in comparison to wild type, to convert externally supplied Glc-1-P into MOS. PHO1-repressed tubers were unable to generate glucans since almost no difference was obtained when subtracting the relative amount obtained from treatment samples incubated with Glc-1-P minus control samples (Figure 3.4). Nevertheless, PHO1-repressed control samples already contained more and longer MOS with a degree of polymerization up to DP30 (Figure 3.5). This inherent MOS content could be explained as an accumulation of highly polymerized glucans in the amyloplast in this transgenic line and points to the function of PHO1 in potato tubers in a depolymerizing direction. The same effect was reported by Malinova et al. (2014) in *Arabidopsis thaliana phs1a* knockout plants lacking the plastidial phosphorylase, in which maltodextrins with a DP up to 10 were detected. In contrast, in wild-type plants maltodextrins whose DP exceeded 4 were scarcely detectable. In that case, the transitory starch metabolism was analyzed, and thus both starch synthesis and degradation processes occurred repeatedly. However, in this case, since discs samples were generated from growing tubers, therefore mainly synthesis of storage starch occurred and the biochemical significance of the increased and longer MOS for the metabolism is not clear. A possible explanation is that the observed MOS were result of the initiation of new starch granules or partial degradation of starch granules during synthesis (e.g., during the trimming of the amylopectin molecules). Since PHO1 activity was repressed in this transgenic line, such trimmed MOS could remain intact. Overall, this was fascinating but needs further investigation.

We found that PHO2-repressed tuber discs incubated in Glc-1-P were able to produce MOS at a comparable level to WT (Figure 3.7 and 3.7). For that reason, a PHO2 connection with the MOS metabolism can be practically excluded. Under these circumstances, we can assume that the detected MOS were localized exclusively in the amyloplasts.

In wild-type and PHO2-repressed discs incubated with Glc-1-P, decreasing proportions short MOS (DP3-5) were detected. Meanwhile, proportion of longer MOS were increased. This

observation also referred to PHO1 as the responsible enzyme for the detected alterations, as this isoform revealed a primer favoritism for short glucans and, specifically in potato, a preference for DP5 has been reported (Kitaoka et al., 2002; Kadokawa, 2018). Remarkably, increased proportions of DP5 were observed both in wild-type and PHO1-repressed tubers when they were exposed to light, thus realizing photosynthesis, in comparison with control tubers where no photosynthetic activity was occurring. Assumptions based on this observation are hard to take over, since the carbohydrate metabolism in green tubers must be drastically changed and a possible activity of PHO1 in the phosphorolytic direction cannot be assumed, since the same effect was observed in tubers with strong repression of this specific enzyme. On the other side and noteworthy, PHO2-repressed tubers revealed an increased PHO1 activity observed in native PAGE assays using potato soluble proteins (Figure 3.3) A possible explanation for this could be that higher expression levels of the plastidial phosphorylase existed in PHO2-repressed plants as a compensation mechanism to its repression in the cytosolic isoform. However, the biological function is not clear. The effect of this higher PHO1 activity in the PHO2-repressed line was clearly detectable in the MOS metabolism following Glc-1-P incubation. Therefore, with increasing incubation time, more MOS were accumulated in the transgenic tuber discs, as compared to wild type (Figure 3.7B), and the MOS revealed small alteration in the chain length (Figure 3.7A). Especially shorter chains (DP4-6) were reduced in amount, as compared to wild-type, and middle long chains (DP9-13) were increased, and thus it may be that the shorter chains had been used for elongation by PHO1 during the Glc-1-P incubation. This agreed with the known substrate specificity of PHO1 that preferred short linear MOS (Kitaoka et al., 2002).

Furthermore, glucosylation mediated through the plastidial phosphorylase immediately occurred once the Glc-1-P was available, as seen after five minutes incubation. This result supports the increasing evidence that a specific transporter for Glc-1-P must exist in the plastidial membranes, so this metabolite could be exchanged between the cytosol and plastid. Recently, Malinova et al. (2020) indicated that two transporters expressed in the membrane, previously described as UDP-galactose/UDP-rhamnose, were able to transport Glc-1-P in *A. thaliana*. Based on these observations, the existence of homologous transporters in *S. tuberosum* L. as well as in other plant species seems highly probable. It is known from the previous starch labelling experiments that the transport efficiency of this hexose phosphate is higher in potato tubers compared to Arabidopsis (Fettke et al., 2010; 2011). This could stem from the possibilities that either the transporters are highly expressed, or they perform

more efficiently. Therefore, some additional Glc-1-P transporters could possibly exist in the heterotrophic cell of potato tubers. With all this evidence, an alternate route including a direct transport of Glc-1-P into the amyloplasts of the sink organs should be considered beyond the established GPT (Glucose-6-phosphate/phosphate translocator). However, evaluation of this Glc-1-P uptake capacity in different plant species would provide wider information concerning this putative specific transporter.

### 7.3 Simultaneous repression of both plastidial and cytosolic PGM did not influence the MOS formation capability

Since phosphoglucomutase (PGM) is an enzyme directly responsible of Glc-1-P regulation in plant metabolism by catalyzing the interconversion of Glc-1-P and Glc-6-P, we hypothesized that a lack of both isoforms should not influence the observed effects on the MOS, as this depends on the direct transport of the supplied Glc-1-P into the cell and amyloplasts with further usage by PHO1. Tuber discs of this transgenic line revealed that the capacity to generate maltodextrins was not affected (Figure 3.9). Only small alterations in the chain length distribution were detected. Therefore, following incubation with Glc-1-P, a lower percentage of DP7–DP9 were present in the PGM transgenic tuber discs, as compared to wild-type. This could be explained by a lack of conversion of applied Glc-1-P to Glc-6-P and thus increasing amounts of the former in the amyloplasts causing an augmented action of PHO1, even though PHO1 activity is unaltered in PGM plants under normal conditions. The results here presented using the transgenic PGM-repressed potato were in accordance with the findings of Fernie et al. (2002), who analyzed the content of starch, Glc-1-P and Glc-6-P in the same potato line repressing the plastidial and cytosolic PGM, resulting in little difference with respect to wild-type. However, the tubers of this transgenic potato revealed the highest MOS amount independent of any incubation (Figure 3.11). The reason remains unclear, but a possibility could be the lack of conversion of Glc-6-P into Glc-1-P following the equilibrium, and therefore, more Glc-1-P was available and used for MOS metabolism. Again, a starch metabolism alteration was more likely, and thus, starch initiation, the inner starch structure or degradation could be massively altered. In addition, the fluxes and the involved metabolites may have played a role, even when the estimated starch amount was similar to wild type (Fernie et al., 2002).

For the observed *in situ* alterations of the MOS metabolism, *in planta* data is still lacking. Thus, it would be interesting to observe whether, under specific conditions, the MOS

metabolism would be affected in a similar way. It has been shown, for instance, that repression of PHO1 did affect starch parameters under low temperatures in maize (Satoh et al., 2008) and potato (Orawetz et al., 2016). In these cases, it is very probable that the MOS metabolism was also influenced. As Glc-1-P has also been detected in the apoplast fraction (Malinova et al., 2020), a transport of this metabolite within the plant was provided and could have a potential biotechnology application to alter the starch or MOS properties in specific tissues or organs.

From the overall data, we concluded that i) a Glc-1-P transporter must exist within the plasma membrane as well as in the amyloplast membrane; ii) when the Glc-1-P/Pi ratio was high, simulated by the addition of Glc-1-P, synthesis of MOS catalyzed by PHO1 occurred, which could successively impact on starch metabolism; and iii) a Glc-6-P independent pathway, and thus also independent of PGM action, could naturally occur to produce maltodextrins with a high degree of polymerization.

# 8 Conclusions

During this research project, bioanalytical techniques were used on the investigation of two different classes of molecules involved in the metabolism of starch. MALDI-TOF and capillary electrophoresis were the principal techniques that were utilized, resulting in practical, precise, and versatile analytical methods that allowed the recognition of proteins and carbohydrates. Proteins identified in this study that were strongly interacting to the potato starch granules corresponded to previously described proteins related to the starch metabolism. Remarkably, GWD and PWD, despite being enzymes commonly associated to the starch degradation, we found them strongly interacting to the starch granules in developing tubers. Based on this observation, we assume that the activity of GWD and PWD is not restricted only to the starch breakdown but is also required during the synthesis of storage starch. However, the specific role and relevance of these enzymes during starch synthesis must be still investigated. On the other hand, proteins that were weakly interacting to the starch granules surface mainly consisted of protease inhibitors having a subcellular location different from plastids. Considering the high expression in potato tubers of such protease inhibitors, we concluded that these proteins were contaminants that were not completely removed from the starch granules during the starch isolation procedure.

On the other hand, we demonstrated that the starch proteome profile is altered during the storage of potato tubers under different temperature conditions. A more profound analysis would be very useful on revealing which specific starch bound proteins are preferentially expressed under specific environmental or stress conditions.

On the second part of the project comprising the analysis of MOS in potato tuber, the results obtained confirmed former evidence regarding the ability of parenchyma cells of potato tuber to incorporate externally supplied Glc-1-P into the plastidial compartment for its utilization. Therefore, we concluded that a specific Glc-1-P transporter must exist both in the plasmatic and amyloplast membrane that allows the transport of Glc-1-P into the amyloplast. We also demonstrated that the plastidial glucan phosphorylase PHO1 is essential in the maltodextrin metabolism and is very efficient on the polymerization of α- 1,4-linked glucans when the concentration of Glc-1-P is augmented in tuber parenchyma cells. Under physiological conditions, PHO1 is required for the degradation of MOS having a high degree of polymerization, which was evident on the exceptional accumulation of long MOS detected in transgenic plants repressing this enzyme. Considering all these previous

statements, we reached the conclusion that an alternative maltodextrin and starch metabolic route independent of the Glc-6-P pathway, and therefore also from the action PGM exists in potato tubers.

# 9 References

**Abt, M. R., Pfister, B., Sharma, M., Eicke, S., Bürgy, L., Neale, I., Seung, D., & Zeeman, S. C. (**2020) STARCH SYNTHASE5, a noncanonical starch synthase-like protein, promotes starch granule initiation in Arabidopsis. *The Plant cell*, 32(8), 2543–2565.

**Adigwe, O. P., Egharevba, H. O., & Emeje, M. O.** (2022) Starch: a veritable natural polymer for economic revolution. *Starch - Evolution and Recent Advances*, 1-15, IntechOpen.

**Albrecht, T., Koch, A., Lode, A., Greve, B., Schneider-Mergener, J., & Steup, M**. (2001) Plastidic (Pho1-type) phosphorylase isoforms in potato (*Solanum tuberosum* L.) plants: expression analysis and immunochemical characterization. *Planta*, 213(4), 602–613.

**Apriyanto, A., Compart, J., & Fettke, J.** (2022) A review of starch, a unique biopolymer - structure, metabolism and in planta modifications. *Plant Science*, 318: 111223.

**Atkinson, M. R., Johnson E., & Morton, R. K**. (1961) Equilibrium constants of phosphoryl transfer from C (1) to C (6) of α D- glucose 1- phosphate and from glucose 6- phosphate to water. *The Biochemical journal*, 79 (1), 12-15.

**Ball, S., Guan, H. P., James, M., Myers A., Keeling, P., Mouille, G., Buléon, A., Colonna, P., & Preiss, J.** (1996) From glycogen to amylopectin: a model for the biogenesis of the plant starch granule. *Cell*. 9;86 (3):349-52.

**Bancel, E., Rogniaux, H., Debiton, C., Chambon, C., & Branlard, G**. (2010) Extraction and proteome analysis of starch granule-associated proteins in mature wheat kernel (*Triticum aestivum* L.). *Journal of proteome research*, 9(6), 3299–3310.

**Bogracheva, T. Y., Morris, V. J., Ring, S. G., & Hedley, C. L.** (1998) The granular structure of C-type pea starch and its role in gelatinization. *Biopolymers*, *45*, 323-332.

**Bradford, M.** (1976) A rapid and sensitive method for the quantitation of microgram quantities of protein utilizing the principle of protein-dye binding. *Analytical biochemistry*, *72*, 248–254.

**Braun, D. M., Wang, L., & Ruan, Y. L.** (2014) Understanding and manipulating sucrose phloem loading, unloading, metabolism, and signaling to enhance crop yield and food security. *Journal of experimental botany*, *65*(7), 1713–1735.

**Brust, H., Orzechowski, S., Fettke, J., & Steup, M.** (2013) Starch synthesizing reactions and paths: *in vitro* and *in vivo* studies. *Journal of Applied Glycoscience*, 60, 3–20.

**Buléon, A., Colonna, P., Planchot, V., & Ball, S.** (1998) Starch granules: structure and biosynthesis. *International journal of biological macromolecules*, *23*(2), 85–112.

**Chen, L. Q.** (2014) SWEET sugar transporters for phloem transport and pathogen nutrition. *New Phytologist*, 201: 1150-1155.

**Chia, T., Thorneycroft, D., Chapple, A., Messerli, G., Chen, J., Zeeman, S. C., Smith, S. M., & Smith, A. M.** (2004) A cytosolic glucosyltransferase is required for conversion of starch to sucrose in Arabidopsis leaves at night. *The Plant journal: for cell and molecular biology*, *37*(6), 853–863.

**Cho, M. H., Lim, H., Shin, D. H., Jeon, J. S., Bhoo, S. H., Park, Y. I., & Hahn, T. R.** (2011) Role of the plastidic glucose translocator in the export of starch degradation products from the chloroplasts in Arabidopsis thaliana. *The New phytologist*, *190*(1), 101–112.

**Cuesta-Seijo, J. A., Nielsen, M. M., Ruzanski, C., Krucewicz, K., Beeren, S. R., Rydhal, M. G., Yoshimura, Y., Striebeck, A., Motawia, M. S., Willats, W. G., & Palcic, M. M.** (2016) In vitro biochemical characterization of all barley endosperm starch synthases. *Frontiers in plant science*, 6, 1265.

**Delatte, T., Umhang, M., Trevisan, M., Eicke, S., Thorneycroft, D., Smith, S. M., & Zeeman, S. C.** (2006) Evidence for distinct mechanisms of starch granule breakdown in plants. *The Journal of biological chemistry*, 281(17), 12050–12059.

**Delvallé, D., Dumez, S., Wattebled, F., Roldán, I., Planchot, V., Berbezy, P., Colonna, P., Vyas, D., Chatterjee, M., Ball, S., Mérida, A., & D'Hulst, C.** (2005) Soluble starch synthase I: a major determinant for the synthesis of amylopectin in Arabidopsis thaliana leaves. *The Plant journal: for cell and molecular biology*, *43*(3), 398–412.

**Egli, B., Kölling, K., Köhler, C., Zeeman, S. C. & Streb, S.** (2010) Loss of cytosolic phosphoglucomutase compromises gametophyte development in Arabidopsis. *Plant physiology*, *154*(4), 1659–1671.

**Feike, D., Seung, D., Graf, A., Bischof, S., Ellick, T., Coiro, M., Soyk, S., Eicke, S., Mettler-Altmann, T., Lu, K. J., Trick, M., Zeeman, S. C., & Smith, A. M.** (2016) The starch granule-associated Protein EARLY STARVATION1 is required for the control of starch degradation in Arabidopsis thaliana leaves. *The Plant cell*, *28*(6), 1472–1489.

**Fernie A. R., Roessner, U., Trethewey, R. N. & Willmitzer, L.** (2001) The contribution of plastidial phosphoglucomutase to the control of starch synthesis within the potato tuber. *Planta*. Jul;213(3):418-26.

**Fernie, A. R., Bachem, C. W. B., Helariutta, Y., Neuhaus, H. E., Prat, S., Ruan, Y. L., Stitt, M., Sweetlove, L. J., Tegeder, M., Wahl, V., Sonnewald, S., & Sonnewald, U.** (2020) Synchronization of developmental, molecular and metabolic aspects of source-sink interactions. *Nature plants*, 6(2), 55–66.

**Fernie, A. R., Swiedrych, A., Tauberger, E., Lytovchenko, A., Trethewey, R. N., & Willmitzer, L**. (2002) Potato plants exhibiting combined antisense repression of cytosolic and plastidial isoforms of phosphoglucomutase surprisingly approximate wild type with respect to the rate of starch synthesis, *Plant Physiology and Biochemistry*, Volume 40, Issue 11, Pages 921-927.

**Fettke J.**, **Eckermann, N., Poeste, S., Pauly, M., & Steup, M**. (2004) The glycan substrate of the cytosolic (Pho 2) phosphorylase isozyme from *Pisum sativum* L.: identification, linkage analysis and subcellular localization. *Plant Journal*. 39: 933-946.

**Fettke, J., Albrecht, T., Hejazi, M., Mahlow, S., Nakamura, Y., & Steup, M.** (2010) Glucose 1-phosphate is efficiently taken up by potato (Solanum tuberosum) tuber parenchyma cells and converted to reserve starch granules. *The New phytologist*, 185(3), 663–675.

**Fettke, J., Chia, T., Eckermann, N., Smith, A., & Steup, M.** (2006) A transglucosidase necessary for starch degradation and maltose metabolism in leaves at night acts on cytosolic heteroglycans (SHG). *The Plant journal: for cell and molecular biology*, 46(4), 668–684.

**Fettke, J., Malinova, I., Albrecht, T., Hejazi, M., & Steup, M.** (2011) Glucose-1-phosphate transport into protoplasts and chloroplasts from leaves of Arabidopsis. *Plant physiology*, 155(4), 1723–1734.

**Fettke, J., Nunes-Nesi, A., Alpers, J., Szkop, M., Fernie, A. R. & Steup, M**. (2008) Alterations in cytosolic glucose phosphate metabolism affect structural features and biochemical properties of starch-related heteroglycans. *Plant Physiology*. 148: 1614-1629.

**Fettke, J., Poeste, S., Eckermann, N., Tiessen, A., Pauly, M., Geigenberger, P., & Steup, M.** (2005) Analysis of cytosolic heteroglycans from leaves of transgenic potato (Solanum tuberosum L.) plants that under- or overexpress the Pho 2 phosphorylase isozyme. *Plant & cell physiology*, 46(12), 1987–2004.

**Castellanos, J. & Fettke, J.** (2022) The plastidial glucan phosphorylase affects the maltooligosaccharide metabolism in parenchyma cells of potato (*Solanum tuberosum* L.) tuber discs. *Plant & cell physiology*, pcac174.

**Green, A. R., Nissen, M. S., Kumar, G. N., Knowles, N. R., & Kang, C.** (2013) Characterization of *Solanum tuberosum* multicystatin and the significance of core domains. *Plant Cell*. Dec;25(12):5043-52.

**Grimaud, F., Rogniaux, H., James, M. G., Myers, A. M., & Planchot, V.** (2008) Proteome and phosphoproteome analysis of starch granule-associated proteins from normal maize and mutants affected in starch biosynthesis. *Journal of experimental botany*, *59*(12), 3395–3406.

**Guedon, E., Desvaux, M., & Petitdemange, H.** (2000) Kinetic analysis of *Clostridium cellulolyticum* carbohydrate metabolism: importance of glucose 1-phosphate and glucose 6-phosphate branch points for distribution of carbon fluxes inside and outside cells as revealed by steady-state continuous culture. *Journal of bacteriology*, 182(7), 2010–2017.

**Hanes, C.** (1940) The reversible formation of starch from glucose-1- phosphate catalyzed by potato phosphorylase. *Proceedings of the Royal Society of London*. Series B - Biological Sciences, 129, 174 - 208.

**Helle, S., Bray, F., Putaux, J. L., Verbeke, J., Flament, S., Rolando, C., D'Hulst, C., & Szydlowski, N.** (2019) Intra-sample heterogeneity of potato starch reveals fluctuation of starch-binding proteins according to granule morphology. *Plants* (Basel, Switzerland), 8(9), 324.

**Helle, S., Bray, F., Verbeke, J., Devassine, S., Courseaux, A., Facon, M., Tokarski, C., Rolando, C., & Szydlowski, N.** (2018) Proteome analysis of potato starch reveals the presence of new starch metabolic proteins as well as multiple protease inhibitors. *Frontiers in plant science*, *9*, 746.

**Hirsch, C. D., Hamilton, J. P., Childs, K. L., Cepela, J., Crisovan, E., Vaillancourt, B., Hirsch, C. N., Habermann, M., Neal, B., & Buell, C. R.** (2014) Spud DB: a resource for mining sequences, genotypes, and phenotypes to accelerate potato breeding. *The Plant Genome*, 7(1).

**Hizukuri, S., Kaneko, T. & Takeda, Y.** (1983) Measurement of the chain length of amylopectin and its relevance to the origin of crystalline polymorphism of starch granules. *Biochimica et Biophysica Acta*, 760, 188-191.

**Hofius, D. & Börnke, F**. (2007) Photosynthesis, carbohydrate metabolism and source–sink relations. In *Potato Biology and Biotechnology: Advances and Perspectives*. D. Vreugdenhil (ed). Elsevier. Pp. 257-285.

**Hwang, P., Koper, K., & Okita, T. W**. (2020) The plastid phosphorylase as a multiple-role player in plant metabolism. *Plant Science*.,2 90, 110303.

**Hwang, S. K., Koper, K., Satoh, H., & Okita, T. W.** (2016) Rice endosperm starch phosphorylase (Pho1) assembles with disproportionating enzyme (Dpe1) to form a protein complex that enhances synthesis of malto-oligosaccharides. *The Journal of biological chemistry*, *291*(38), 19994–20007.

**Imberty, A. & Perez, S. (**1988) A revisit to the three-dimensional structure of B-type starch. *Biopolymers*, 27, 1205-1221.

**Ishikawa, A., Ohta, S., Matsuoka, K., Hattori, T. & Nakamura, K**. (1994) A family of potato genes that encode Kunitz-type proteinase inhibitors: structural comparisons and differential expression. *Plant & cell physiology*, 35(2):303-312.

**Jørgensen, M., Bauw, G., & Welinder, K. G**. (2006) Molecular properties and activities of tuber proteins from starch potato cv. Kuras. *Journal of agricultural and food chemistry*, *54*(25), 9389–9397.

**Julius, B. T., Leach, K., Tran, T., Mertz, R. & Braun, D.** (2017) Sugar transporters in plants: new insights and discoveries, *Plant and Cell Physiology*, Volume 58, Issue 9, Sep, 1442–1460.

**Kadokawa, J.** (2018) α-Glucan phosphorylase-catalyzed enzymatic reactions using analog substrates to synthesize non-natural oligo- and polysaccharides. *Catalysts* 8, no. 10: 473.

**Kammerer, B., Fischer, K., Hilpert, B., Schubert, S., Gutensohn, M., Weber, A., & Flügge, U. I**. (1998) Molecular characterization of a carbon transporter in plastids from heterotrophic tissues: the glucose 6-phosphate/phosphate antiporter. *The Plant cell*, *10*(1), 105–117.

**Kirchberger, S., Leroch, M., Huynen, M. A., Wahl, M., Neuhaus, H. E., & Tjaden, J.** (2007) Molecular and biochemical analysis of the plastidic ADP-glucose transporter (ZmBT1) from *Zea mays*. *The Journal of biological chemistry*, *282*(31), 22481–22491.

**Kitaoka, M. & Hayashi, K**. (2002) Carbohydrate-processing phosphorolytic enzymes. *Trends in glycoscience and glycotechnology*. 14:35–50.

**Koch K. E.** (1996) Carbohydrate-modulated gene expression in plants**.** *Annual review of plant physiology and plant molecular biology*, 47, 509–540.

**Lin, Q., Facon, M., Putaux, J. L., Dinges, J. R., Wattebled, F., D'Hulst, C., Hennen-Bierwagen, T. A., & Myers, A. M**. (2013) Function of isoamylase-type starch debranching enzymes ISA1 and ISA2 in the *Zea mays* leaf. *The New phytologist*, 200(4), 1009–1021.

**Lin, Y. C., Chang, S. C. & Juang, R. H.** (2017) Plastidial α-glucan phosphorylase 1 complexes with disproportionating enzyme 1 in *Ipomoea batatas* storage roots for elevating malto-oligosaccharide metabolism. *PLoS One*. May 4;12(5): e0177115.

**Lloyd, J. R. & Kossmann, J.** (2015) Transitory and storage starch metabolism: Two sides of the same coin? *Current opinion in biotechnology*, 32: 143–148.

**Lorberth, R., Ritte, G., Willmitzer, L., & Kossmann, J.** (1998) Inhibition of a starch-granule-bound protein leads to modified starch and repression of cold sweetening. *Nature biotechnology*, *16*(5), 473–477.

**Lytovchenko, A., Bieberich, K., Willmitzer, L. & Fernie A. R.** (2002) Carbon assimilation and metabolism in potato leaves deficient in plastidial phosphoglucomutase. *Planta* 215, 802–811.

**MacNeill, G. J., Mehrpouyan, S., Minow M. A., Patterson, J., Tetlow, I. J. & Emes, M. J.** (2017) Starch as a source, starch as a sink: the bifunctional role of starch in carbon allocation, *Journal of Experimental Botany*, Volume 68, Issue 16, 3 October, Pp.4433–4453.

**Mahlow, S., Hejazi, M., Kuhnert, F., Garz, A., Brust, H., Baumann, O., & Fettke, J.** (2014) Phosphorylation of transitory starch by α-glucan, water dikinase during starch turnover affects the surface properties and morphology of starch granules. *The New phytologist*, 203(2), 495–507.

**Mahlow, S., Orzechowski, S., & Fettke, J**. (2016) Starch phosphorylation: insights and perspectives. *Cellular and molecular life sciences*: *CMLS*, 73(14), 2753–2764. https://doi.org/10.1007/s00018-016-2248-4.

**Malinova, I., Kössler, S., Orawetz, T., Matthes, U., Orzechowski, S., Koch, A., & Fettke, J**. (2020) Identification of two Arabidopsis thaliana plasma membrane transporters able to transport glucose-1-phosphate. *Plant & cell physiology*, *61*(2), 381–392.

**Malinova, I., Kunz, H. H., Alseekh, S., Herbst, K., Fernie, A. R., Gierth, M., & Fettke, J.** (2014) Reduction of the cytosolic phosphoglucomutase in Arabidopsis reveals impact on plant growth, seed and root development, and carbohydrate partitioning. *PloS one*, 9(11), e112468.

**Malinova, I., Mahlow, S., Alseekh, S., Orawetz, T., Fernie, A. R., Baumann, O., Steup, M., & Fettke, J.** (2014) Double knock-out mutants of Arabidopsis thaliana grown under normal conditions reveal that the plastidial phosphorylase isozyme (PHS1) participates in transitory starch metabolism. *Plant Physiology*. 164: 907-921.

**Merida, A. & Fettke, J.** (2021) Starch granule initiation in *Arabidopsis thaliana* chloroplasts. *The Plant journal: for cell and molecular biology*, 107: 688-697.

**Myers, A. M., Morell, M. K., James, M. G., & Ball, S. G.** (2000) Recent progress toward understanding biosynthesis of the amylopectin crystal. *Plant physiology*, *122*(4), 989–997.

**Naeem, M., Tetlow, I. and Emes, M.** (1997) Starch synthesis in amyloplasts purified from developing potato tubers. *Plant journal*, 11: 1095-1103.

**Nakamura, T., Yamamori, M., Hirano, H., Hidaka, S., & Nagamine, T.** (1995) Production of waxy (amylose-free) wheats. *Molecular & general genetics: MGG*, *248*(3), 253–259.

**Nielsen, T. H., Wischmann, B., Enevoldsen, K., & Møller, B. L.** (1994) Starch phosphorylation in potato tubers proceeds concurrently with de novo biosynthesis of starch. *Plant Physiology.* 105, 111– 117.

**Nissen, M. S., Kumar, G. N., Youn, B., Knowles, D. B., Lam, K. S., Ballinger, W. J., Knowles, N. R. & Kang, C.** (2009) Characterization of *Solanum tuberosum* multicystatin and its structural comparison with other cystatins. *Plant Cell*, 21: 861–875.

**Orawetz, T., Malinova, I., Orzechowski, S., & Fettke, J.** (2016) Reduction of the plastidial phosphorylase in potato (*Solanum tuberosum* L.) reveals impact on storage starch structure during growth at low temperature. *Plant physiology and biochemistry*, 100: 141-149.

**Pérez, S. & Bertoft, E.** (2010) The molecular structures of starch components and their contribution to the architecture of starch granules: a comprehensive review. *Starch/Staerke*, 62, 389-420.

**Pfister, B., & Zeeman, S. C.** (2016) Formation of starch in plant cells. *Cellular and molecular life sciences: CMLS*, *73*(14), 2781–2807.

**Pouvreau, L., Gruppen, H., Piersma, S. R., van den Broek, L. A. M, van Koningsveld, G. A., & Voragen, A. G.** (2001) Relative abundance and inhibitory distribution of protease inhibitors in potato juice from cv. Elkana. *Journal of Agricultural and Food Chemistry49* (6), 2864-2874.

**Pouvreau, L., Gruppen, H., Van Koningsveld, G. A., Van Den Broek, L. A., & Voragen, A. G.** (2003) The most abundant protease inhibitor in potato tuber (cv. Elkana) is a serine protease inhibitor from the Kunitz family. *Journal of agricultural and food chemistry*, *51*(17), 5001–5005.

**Proels R. K. & Hückelhoven, R.** (2014) Cell-wall invertases, key enzymes in the modulation of plant metabolism during defence responses. *Molecular plant pathology*. 15(8):858-64.

**Rodis P. & Hoff J. E.** (1984) Naturally occurring protein crystals in the potato: Inhibitor of papain, chymopapain, and ficin. *Plant physiol*ogy, 74: 907–911.

**Santelia, D., & Lunn, J. E.** (2017) Transitory starch metabolism in guard cells: unique features for a unique function, *Plant Physiology*, Volume 174, Issue 2, 539–549.

**Satoh, H., Shibahara, K., Tokunaga, T., Nishi, A., Tasaki, M., Hwang, S. K., Okita, T. W., Kaneko, N., Fujita, N., Yoshida, M., Hosaka, Y., Sato, A., Utsumi, Y., Ohdan, T., & Nakamura,**

**Y.** (2008) Mutation of the plastidial alpha-glucan phosphorylase gene in rice affects the synthesis and structure of starch in the endosperm. *The Plant cell*, *20* (7), 1833–1849.

**Sawada, T., Itoh, M., & Nakamura, Y.** (2018) Contributions of three starch branching enzyme isozymes to the fine structure of amylopectin in rice endosperm. *Frontiers in plant science*, 9, 1536.

**Seung, D., Boudet, J., Monroe, J., Schreier, T. B., David, L. C., Abt, M., Lu, K. J., Zanella, M., & Zeeman, S. C.** (2017) Homologs of PROTEIN TARGETING TO STARCH control starch granule initiation in Arabidopsis leaves. *The Plant cell*, 29 1657–1677.

**Shevchenko, A., Wilm, M., Vorm, O., & Mann, M.** (1996) Mass spectrometric sequencing of proteins silver-stained polyacrylamide gels. *Analytical chemistry*, *68*(5), 850–858.

**Shoaib, N., Liu, L., Ali, A., Mughal, N., Yu, G., & Huang, Y.** (2021) Molecular functions and pathways of plastidial starch phosphorylase (PHO1) in starch metabolism: current and future perspectives. *International journal of molecular sciences*, *22*(19), 10450.

**Singh, A., Compart, J., Al Rawi, S., Mahto, H., Ahmad, A., & Fettke, J**. (2022) LIKE EARLY STARVATION alters the glucan structures at the starch granule surface and thereby influences the action of both starch-synthesizing and -degrading enzymes. *The Plant journal: for cell and molecular biology*, 111(3), 819–835.

**Sonnewald, U., Basner, A., Greve, B. & Steup, M.** (1995) A second L-type isozyme of potato glucan phosphorylase: cloning, antisense inhibition and expression analysis. *Plant molecular biology*, 27(3):567-76.

**Steup, M**. (1988) Starch degrading enzymes. In: Preiss J, editor. *Biochemistry of plants*. Carbohydrates. New York: Academic Press;.p. 255.

**Steup, M.** (1990) Starch degrading enzymes. *Methods in Plant Biochemistry*, Vol. 3. Edited by Lea, P.J. pp. 103–128. Academic Press, London.

**Stiekema, W. J., Heidekamp, F., Dirkse, W. G., van Beckum, J., de Haan, P., Bosch, C. T., & Louwerse, J. D**. (1988) Molecular cloning and analysis of four potato tuber mRNAs. *Plant molecular biology*, *11*(3), 255–269.

**Stitt, M., & Zeeman, S. C.** (2012) Starch turnover: pathways, regulation and role in growth. *Current opinion in plant biology*, 15(3): 282–292.

**Streb, S. & Zeeman, S. C**. (2014) Replacement of the endogenous starch debranching enzymes ISA1 and ISA2 of Arabidopsis with the rice orthologs reveals a degree of functional conservation during starch synthesis. *PLoS One*. Mar 18;9(3): e92174.

**Tauberger, E., Fernie, A. R., Emmermann, M., Renz, A., Kossmann, J., Willmitzer, L., & Trethewey, R. N.** (2000) Antisense inhibition of plastidial phosphoglucomutase provides compelling evidence that potato tuber amyloplasts import carbon from the cytosol in the form of glucose-6-phosphate. *The Plant journal: for cell and molecular biology*, *23*(1), 43–53.

**Tetlow, I. J.** (2018) Starch biosynthesis in crop plants**.** *Agronomy 8*, 81.

**Tetlow, I. J. & Bertoft, E.** (2020) A review of starch biosynthesis in relation to the building block-backbone model. *International journal of molecular sciences*, 21(19), 7011.

**Tetlow, I. J., Wait, R., Lu, Z., Akkasaeng, R., Bowsher, C. G., Esposito, S., Kosar-Hashemi, B., Morell, M. K., & Emes, M. J.** (2004) Protein phosphorylation in amyloplasts regulates starch branching enzyme activity and protein-protein interactions. *The Plant cell*, 16 (3):694-708.

**Tewari, Y. B., Steckler, D. K., & Goldberg, R. N.** (1988) Thermodynamics of isomerization reactions involving sugar phosphates. *The Journal of biological chemistry*, *263*(8), 3664–3669.

**Tickle, P., Burrell, M. M., Coates, S.A., Emes, M.J., Tetlow, I.J., & Bowsher, C.G.** (2009) Characterization of plastidial starch phosphorylase in *Triticum aestivum* L. endosperm. *Journal of plant physiol*ogy, 166, 1465–1478.

**Toinga-Villafuerte, S., Vales, M. I., Awika, J. M., & Rathore, K. S.** (2022) CRISPR/Cas9-mediated mutagenesis of the granule-bound starch synthase gene in the potato variety Yukon Gold to obtain amylose-free starch in tubers. *International journal of molecular sciences*, 23, 4640.

**Turgeon, R. & Ayre, B.** (2005) Pathways and mechanisms of phloem loading. *In Physiological Ecology, Vascular Transport in Plants*. Academic Press, 45-67.

**Van Harsselaar, J. K., Lorenz, J., Senning, M., Sonnewald, U., & Sonnewald, S**. (2017) Genome-wide analysis of starch metabolism genes in potato (*Solanum tuberosum* L.). *BMC Genomics* 18:37.

**Waffenschmidt, S., & Jaenicke, L.** (1987) Assay of reducing sugars in the nanomole range with 2,2'-bicinchoninate. *Analytical biochemistry*, *165*(2), 337–340.

**Wang, Y., Zhang, H., Li, Y., Zhang, Q., Liu, Q., Zhai, H., Zhao, N., Yang, Y., & He, S.** (2022) Plastidial phosphoglucomutase (pPGM) overexpression increases the starch content of transgenic sweet potato storage roots. *Genes*, 13(12), 2234.

**Webster, J., & Oxley, D.** (2012) Protein identification by MALDI-TOF mass spectrometry. *Methods in molecular biology (Clifton, N.J.)*; 800:227-240.

**Xing, S., Meng, X., Zhou, L., Mujahid, H., Zhao, C., Zhang, Y., Wang, C., & Peng, Z.** (2016) Proteome profile of starch granules purified from rice (*Oryza sativa*) endosperm**.** *PloS one***,** 11(12), e0168467.

**Zhang, P., & Hamaker, B. R.** (2012) Banana starch structure and digestibility. *Carbohydrate Polym*er, 87, 1552–1558.

**Zhang, X., Szydlowski, N., Delvallé, D., D'Hulst, C., James, M. G., & Myers, A. M.** (2008) Overlapping functions of the starch synthases SSII and SSIII in amylopectin biosynthesis in Arabidopsis. *BMC plant biology*, 8, 96.

## 9.1 Online resources

**AlphaFold Protein Structure Database**. Available in: https://alphafold.ebi.ac.uk/

**Mascot** database from Matrix Science (2021). Available in: https://matrixscience.com

**PeptideMass** from Expasy Swiss Bioinformatics Resource. Available in: https://web.expasy.org/peptide_mass/

**Spud DB Potato Genomics Resource** (2022). Available in: plantbiology.solanaceae.msu.edu